ref. 32) and showed that drugs with similar modes of actions were classified into the same cluster by hierarchical clustering (19). In this study, we constructed a new panel of 45 human cancer cell lines (JFCR-45), comprising cancer cell lines derived from tumors from three different organ types: breast, liver, and stomach. In particular, the inclusion of cell lines derived from gastric and hepatic cancers is a major point of novelty. JFCR-45 can be used for analyzing both organ-specific differences in chemosensitivity and intraorgan heterogeneity of chemosensitivity. We examined 53 anticancer drugs for their activity against JFCR-45 and observed differential activity across the whole panel as well as within a single organ type (e.g., breast, liver, or stomach). Furthermore, as shown in Fig. 1, using JFCR-45, drugs with a similar mode of action (such as a tubulin binder or topo I inhibitor) were classified into the same cluster, which were the same as the clusters established for NCI-60 (35) and JFCR-39 (19). These results suggest that the cell line panel-based assessment system is generally effective for classifying anticancer drugs with the same modes of action into the same set of clusters.

In this study, we investigated the gene expression profiles of 42 cell lines of JFCR-45 using cDNA array consisting of 3,537 genes. Hierarchical clustering analysis of these gene expression profiles classified organ-specific cell lines mostly into the same cluster, suggesting that these cell lines maintained the genetic characteristics of the parent organ as far as the gene expression profiles were concerned.

We did a Pearson correlation analysis of the gene expression database and the drug sensitivity database. Consequently, many genes whose expressions were correlated with respect to the sensitivity of each drug were identified. For example, DNA alkylating agents and nucleic acid–related genes, including *SF1* encoding ZFM1, *c-JUN* oncogene, and *SFRS9* were extracted as the genes sensitive to MMC. The genes that were sensitive to paclitaxel included tubulin binder and cytoskeleton-related genes, such as *VIL2* encoding ezrin and *ACTB* encoding β-actin.

These results suggest that the extracted genes are the predictive markers of drug efficacy. We further applied Pearson correlation analysis to each type (i.e., breast, liver, or stomach cancer) of cell lines. There were two advantages in this type of analysis: one is that we could compare the cell lines having the same organ background and another is that organ-specific genes, which worked as the sensitive or resistant factors, could be extracted. For example, for MMC, several genes (such as *INHBB*, *NK4*, and *HSPA1A*) were newly extracted as candidate genes sensitive to MMC from the breast cancer cell lines. Surprisingly, compared with the breast and liver cancer cells, many new candidate genes were extracted from the stomach cancer cell lines. These extracted genes were considered as the candidates for organ-specific predictive markers of drug efficacy.

We hypothesized that some of the candidate sensitivity genes described above might causally affect the chemosensitivity of cancer cell lines. To validate this possibility, we selected 19 genes, including *HSPA1A*, *JUN*, and *IL-18*, and examined whether the expression of these candidate genes would affect the cellular sensitivity to anticancer drugs. Overexpression of 2 of the 19 genes, *HSPA1A* encoding 70-kDa heat shock protein and *JUN* encoding c-JUN, indeed enhanced cellular sensitivity to MMC in HT1080 cells (Fig. 3), suggesting that they function to mediate MMC sensitivity. This was an unexpected finding, because a direct relationship between these two genes and MMC sensitivity has not been reported previously, although a relationship between heat shock protein and cancer has been suggested previously (36, 37). How these two genes potentiate MMC sensitivity remains to be clarified. In this validation, we used the HT1080 cell line instead of those in JFCR-45 because of its high transfection efficiency. As the alteration of chemosensitivity following the overexpression of any particular gene may depend highly on the genotypic/phenotypic background of the transfected HT1080 cells, further validation using cell lines within JFCR-45 will be required. In addition to the overexpression experiments, validation by silencing chemosensitivity-related genes using small interfering RNA will be required.

Pioneering attempts to discover new leads and targets and to investigate new aspects of the molecular pharmacology of anticancer drugs by mining the NCI-60 database have been done (31, 33–35). Recently, Szakacs et al. (38) have identified interesting compounds whose activity is potentiated by the MDR1 multidrug transporter. Our previous studies using JFCR-39 (19, 20, 31) and the present study using JFCR-45 also indicate that a comprehensive analysis of chemosensitivity and gene expression data followed by experimental validation leads to the identification of genes that determine drug sensitivity.

In conclusion, we established a sensitivity database for JFCR-45, which focused on organ origin, to 53 anticancer drugs. Using JFCR-45, anticancer drugs were classified according to their modes of action. Moreover, we established a database of the gene expression profiles in 42 cell lines of JFCR-45. Using these two databases, we have identified several genes that may predict chemosensitivity of cancer. Among these candidate genes, we identified two genes, *HSPA1A* and *JUN*, which determined sensitivity to MMC. Thus, this approach is useful not only to discover predictive markers for the efficacy of anticancer drugs but also to discover genes that determine chemosensitivity.

Acknowledgments

We thank Yumiko Mukai, Yumiko Nishimura, Mariko Seki, and Fujiko Ohashi for the determination of chemosensitivity and Dr. Munetika Enjoji (Department of Internal Medicine, National Kyushu Cancer Center, Fukuoka, Japan) for providing the RBE and SSP-25 cell lines.

References

1. Chen CJ, Clark D, Ueda K, et al. Genomic organization of the human multidrug resistance (MDR1) gene and origin of P-glycoproteins. J Biol Chem 1990;265:506–14.

2. Taniguchi K, Wada M, Kohno K, et al. A human canalicular multispecific organic anion transporter (cMOAT) gene is overexpressed in cisplatin-resistant human cancer cell lines with decreased drug accumulation. Cancer Res 1996;56:4124–9.

3. Kool M, de Haas M, Scheffer GL, et al. Analysis of expression of cMOAT (MRP2), MRP3, MRP4, and MRP5, homologues of the multidrug

resistance-associated protein gene (MRP1), in human cancer cell lines. Cancer Res 1997;57:3537–47.

4. Patterson LH, Murray GI. Tumour cytochrome *P*450 and drug activation. Curr Pharm Des 2002;8:1335–47.

5. Batist G, Tulpule A, Sinha BK, et al. Overexpression of a novel anionic glutathione transferase in multidrug-resistant human breast cancer cells. J Biol Chem 1986;261:15544–9.

6. Meisel P. Arylamine *N*-acetyltransferases and drug response. Pharmacogenomics 2002;3:349–66.

7. Nair MG, Baugh CM. Synthesis and biological evaluation of poly-γ-glutamyl derivatives of methotrexate. Biochemistry 1973;12:3923–7.

8. Schimke RT. Methotrexate resistance and gene amplification. Mechanisms and implications. Cancer 1986;57:1912–7.

9. Pinedo HM, Peters GF. Fluorouracil: biochemistry and pharmacology. J Clin Oncol 1988;6:1653–64.

10. Eastman A. Mechanisms of resistance to cisplatin. Cancer Treat Res 1991;57:233–49.

11. Cohen SS. The mechanisms of lethal action of arabinosyl cytosine (araC) and arabinosyl adenine (araA). Cancer 1977;40:509–18.

12. Gustafson DL, Pritsos CA. Enhancement of xanthine dehydrogenase mediated mitomycin C metabolism by dicumarol. Cancer Res 1992;52:6936–9.

13. Kang HC, Kim IJ, Park JH, et al. Identification of genes with differential expression in acquired drug-resistant gastric cancer cells using high-density oligonucleotide microarrays. Clin Cancer Res 2004;10:272–84.

14. Sato T, Odagiri H, Ikenaga SK, et al. Chemosensitivity of human pancreatic carcinoma cells is enhanced by IκBα super-repressor. Cancer Sci 2003;94:467–72.

15. Zembutsu H, Ohnishi Y, Tsunoda T, et al. Genome-wide cDNA microarray screening to correlate gene expression profiles with sensitivity of 85 human cancer xenografts to anticancer drugs. Cancer Res 2002;62:518–27.

16. Okutsu J, Tsunoda T, Kaneta Y, et al. Prediction of chemosensitivity for patients with acute myeloid leukemia, according to expression levels of 28 genes selected by genome-wide complementary DNA microarray analysis. Mol Cancer Ther 2002;1:1035–42.

17. Tanaka T, Tanimoto K, Otani K, et al. Concise prediction models of anticancer efficacy of 8 drugs using expression data from 12 selected genes. Int J Cancer 2004;111:617–26.

18. Scherf U, Ross DT, Waltham M, et al. A gene expression database for the molecular pharmacology of cancer. Nat Genet 2000;24:236–44.

19. Dan S, Tsunoda T, Kitahara O, et al. An integrated database of chemosensitivity to 55 anticancer drugs and gene expression profiles of 39 human cancer cell lines. Cancer Res 2002;62:1139–47.

20. Dan S, Shirakawa M, Mukai Y, et al. Identification of candidate predictive markers of anticancer drug sensitivity using a panel of human cancer cell lines. Cancer Sci 2003;94:1074–82.

21. Kurebayashi J, Kurosumi M, Sonoo H. A new human breast cancer cell line, KPL-3C, secretes parathyroid hormone-related protein and produces tumours associated with microcalcifications in nude mice. Br J Cancer 1996;74:200–7.

22. Shiu RP. Processing of prolactin by human breast cancer cells in long term tissue culture. J Biol Chem 1980;255:4278–81.

23. Engel LW, Young NA, Tralka TS, et al. Establishment and characterization of three new continuous cell lines derived from human breast carcinomas. Cancer Res 1978;38:3352–64.

24. Dor I, Namba M, Sato J. Establishment and some biological characteristics of human hepatoma cell lines. Gann 1975;66:385–92.

25. Tanaka M, Kawamura K, Fang M, et al. Production of fibronectin by HUH6 C15 cell line established from a human hepatoblastoma. Biochem Biophys Res Commun 1983;110:837–41.

26. Fukutomi M, Enjoji M, Iguchi H, et al. Telomerase activity is repressed during differentiation along the hepatocytic and biliary epithelial lineages: verification on immortal cell lines from the same origin. Cell Biochem Funct 2001;19:65–8.

27. Sorimachi K, Hayashi T, Takaoka T, et al. Requirement of serum pretreatment for induction of alkaline phosphatase activity with prednisolone, butyrate, dibutyryl cyclic adenosine monophosphate and NaCl in human liver cells continuously cultured in serum-free medium. Cell Struct Funct 1988;13:1–11.

28. Fujise K, Nagamori S, Hasumura S, et al. Integration of hepatitis B virus DNA into cells of six established human hepatocellular carcinoma cell lines. Hepatogastroenterology 1990;37:457–60.

29. Imanishi K, Yamaguchi K, Suzuki M, et al. Production of transforming growth factor-α in human tumour cell lines. Br J Cancer 1989;59:761–5.

30. Yamori T, Matsunaga A, Sato S, et al. Potent antitumor activity of MS-247, a novel DNA minor groove binder, evaluated by an *in vitro* and *in vivo* human cancer cell line panel. Cancer Res 1999;59:4042–9.

31. Monks A, Scudiero D, Skehan P, et al. Feasibility of a high-flux anticancer drug screen using a diverse panel of cultured human tumor cell lines. J Natl Cancer Inst 1991;83:757–66.

32. Yamori T. Panel of human cancer cell lines provides valuable database for drug discovery and bioinformatics. Cancer Chemother Pharmacol 2003;52 Suppl 1:S74–9.

33. Paull KD, Shoemaker RH, Hodes L, et al. Display and analysis of patterns of differential activity of drugs against human tumor cell lines: development of mean graph and COMPARE algorithm. J Natl Cancer Inst 1989;81:1088–92.

34. Weinstein JN, Kohn KW, Grever MR, et al. Neural computing in cancer drug development: predicting mechanism of action. Science 1992;258:447–51.

35. Weinstein JN, Myers TG, O'Connor PM, et al. An information-intensive approach to the molecular pharmacology of cancer. Science 1997;275:343–9.

36. Laroia G, Cuesta R, Brewer G, et al. Control of mRNA decay by heat shock-ubiquitin-proteasome pathway. Science 1999;284:499–502.

37. Jolly C, Morimoto RI. Role of the heat shock response and molecular chaperones in oncogenesis and cell death. J Natl Cancer Inst 2000;92:1564–72.

38. Szakacs G, Annereau JP, Lababidi S, et al. Predicting drug sensitivity and resistance: profiling ABC transporter genes in cancer cells. Cancer Cell 2004;6:129–37.

Effects of Aryl Hydrocarbon Receptor Signaling on the Modulation of Th1/Th2 Balance[1]

Takaaki Negishi,[2]* Yutaka Kato,* Osamu Ooneda,† Junsei Mimura,† Tomonari Takada,‡ Hidenori Mochizuki,* Masayuki Yamamoto,† Yoshiaki Fujii-Kuriyama,†‡ and Shoji Furusako[2]*

An orally active antiallergic agent, M50367, skews the Th1/Th2 balance toward Th1 dominance by suppressing naive Th cell differentiation into Th2 cells in vitro. Administration results in the suppression of IgE synthesis and peritoneal eosinophilia in vivo. In this report, we determined that M50354 (an active metabolite of M50367) was a ligand for the aryl hydrocarbon receptor (AhR); the immunological effects of this compound on in vitro Th1/Th2 differentiation from naive Th cells and Th1/Th2 balance in vivo were manifested through binding to AhR. These effects were completely abolished in AhR-deficient mice. AhR expression in the naive Th cell was significantly up-regulated by costimulation of TCR and CD28. Suppression of naive Th cell differentiation into Th2 cells via binding of M50354 to AhR was associated with inhibition of GATA-3 expression in Th cells. In addition, forced expression of a constitutively active form of AhR or activation of AhR by the addition of representative ligands suppressed naive Th cell differentiation into Th2 cells. Based on these results, we conclude that AhR functions as a modulator of the in vivo Th1/Th2 balance through activation in naive Th cells. *The Journal of Immunology,* **2005, 175: 7348–7356.**

The aryl hydrocarbon receptor (AhR)[3] is a ligand-activated transcription factor belonging to the basic-helix-loop-helix (bHLH)/period-AhR nuclear translocator-single-minded (PAS) transcription factor superfamily (1). AhR normally exists within the cytoplasm as part of a complex with multiple proteins, including heat shock protein (HSP) 90 (2), AhR-activated 9 (3), and p23 (4). Once a ligand enters the cell and binds AhR, the ligand-bound AhR complex translocates to the nucleus. AhR then forms a heterodimer with another bHLH-PAS protein, AhR nuclear translocator (Arnt), after dissociating from the HSP90-containing complex. Within the nucleus, the AhR/Arnt heterodimer binds to a specific sequence within the promoter of various target genes, designated a xenobiotic responsive element (XRE), to activate their expression (5).

Although the natural ligand of AhR is not known, polycyclic aromatic hydrocarbons, such as 2,3,7,8-tetrachlorodibenzo-*p*-dioxin (TCDD) and related compounds, can bind and activate the AhR. The interaction of these chemicals with AhR mediates a variety of toxic effects, including immune suppression, thymic atrophy, endocrine disruption, tumor promotion, and cell differentiation (6–10). The T cell-mediated immunological response is one of the most sensitive targets of TCDD toxicity (11).

We previously reported that oral administration of the synthetic compound M50367 (Fig. 1) inhibited the production of plasma IgE and pulmonary eosinophilia, resulting in the suppression of airway hyperresponsiveness in murine models of atopic asthma. In ex vivo experiments, while oral administration of M50367 reduced the production of IL-4 and IL-5 by Ag-restimulated splenocytes, it enhanced the production of IFN-γ (12). Treatment of naive Th cells with M50354, a hydrolyzed form of M50367 (Fig. 1), suppressed their in vitro differentiation into Th2 cells with a concomitant increase in the Th1 cell population (13). Thus, the antiallergic effects of this compound may be explained by a direct influence on the Th1/Th2 differentiation of naive Th cells. Although we have found M50367 induces expression of the cytochrome P450 1A1 enzyme (CYP1A1) in mouse liver (our unpublished data), the molecular mechanism underlying this immunomodulatory effect remains unclear.

In this study, we demonstrated that M50354 is an AhR agonist; the AhR signaling pathways activated by M50354 binding skews the Th1/Th2 balance toward Th1 dominance, resulting in immunological responses with antiallergic effects. Furthermore, we determined that the modulatory effects of M50354 on the Th1/Th2 balance were associated with reduced expression of GATA-3, a key factor for Th2 differentiation.

Materials and Methods

Chemicals

M50367 and M50354 (Fig. 1) were synthesized in our laboratory (12). M50354 was used for in vitro studies, and M50367 was used for in vivo studies because M50354 is an active metabolite of M50367 and has low bioavailability (12, 13). [^{3}H]M50354 was synthesized by Amersham Biosciences. 3-Methylcholanthrene (3MC), α-naphthoflavone (αNF), and β-naphthoflavone (βNF) were purchased from Wako Pure Chemical. Resveratrol was obtained from Calbiochem.

Antibodies

Anti-mouse-CD3 (145-2C11), FITC-conjugated anti-CD4 (GK1.5), PE-conjugated anti-IL-4 (11B11), and allophycocyanin-conjugated anti-IFN-γ (XMG1.2) Abs were obtained from BD Pharmingen. An anti-CD28 mAb

*Pharmaceutical Research Center, Mochida Pharmaceutical, Shizuoka, Japan; †Center for Tsukuba Advanced Research Alliance and Institute of Basic Medical Sciences, University of Tsukuba, Tsukuba City, Japan; and ‡Solution Oriented Research for Science and Technology, Japan Science and Technology Agency, Kawaguchi, Japan

Received for publication October 29, 2004. Accepted for publication September 21, 2005.

The costs of publication of this article were defrayed in part by the payment of page charges. This article must therefore be hereby marked *advertisement* in accordance with 18 U.S.C. Section 1734 solely to indicate this fact.

[1] T.T. and Y.F.-K. were supported in part by a grant from Solution Oriented Research and Technology, Japan Science and Technology Agency, Kawaguchi, Japan.

[2] Address correspondence and reprint requests to Dr. Shoji Furusako, Pharmaceutical Research Center, Mochida Pharmaceutical, Shizuoka 412-8524, Japan. E-mail address: furusako@mochida.co.jp

[3] Abbreviations used in this paper: AhR, Aryl-hydrocarbon receptor; bHLH, basic-helix-loop-helix; PAS, period-AhR nuclear translocator-single-minded; XRE, xenobiotic responsive element; Arnt, AhR nuclear translocator; TCDD, 2,3,7,8- tetrachlorodibenzo-*p*-dioxin; 3MC, 3-methylcholanthrene; αNF, α-naphthoflavone; βNF, β-naphthoflavone; CA, constitutively active; wt, wild type; m, murine; PSL, photostimulated luminescence; HPMC, hydroxyl-propyl-methylcellulose; PCB, polychlorinated biphenyl; CYP, cytochrome P-450.

0022-1767/05/$02.00

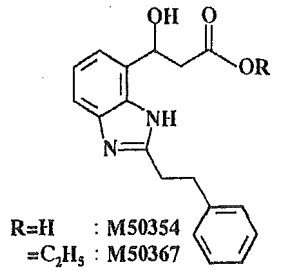

FIGURE 1. Chemical structures of M50354 and M50367.

(PV-1) was purchased from Southern Biotechnology Associates. Microbead-conjugated anti-FITC and anti-CD62L Abs were purchased from Miltenyi Biotec.

Construction of plasmids

A CYP1A1 luciferase reporter plasmid was constructed as follows. A full-length rat *CYP1A1* transcriptional regulatory region (−6300 to +2566) was prepared from pMC6.3k (14) by digestion with *Bgl*II and *Not*I and, after blunting, was end-cloned into the *Sma*I site of the pGL3-Basic vector (Promega) to give pMC6.3k-luc (see Fig. 2*A*).

A recombinant mouse AhR expression vector, wild-type (wt)-murine (m) AhR/pcDNA was constructed as follows. Mouse *AhR* cDNA fragment was amplified from C57BL/6 mouse liver cDNA by using the primers 5′-GGGTCTAGA^{-15}AGGGCGCGGGGCACCATGAG^{+5}-3 and 5′-GGG CTCGAG^{+2463}GAAAACACCTCAACTCTGCACCTTG^{+2427}-3′. The resultant PCR fragment was digested with *Xba*I and *Xho*I, and ligated to the *Xba*I and *Xho*I site of pcDNA3.1$^+$ (Invitrogen Life Technologies).

A constitutively active AhR (CA-AhR) was constructed as described by McGuire et al. (Ref. 15; see Fig. 6*A*). Two cDNA fragments of *AhR*, corresponding to aa 1–276 and 419–805, were amplified by PCR. Primers were designed to carry restriction sites for *Xba*I and *Bam*HI (1–276), and *Bam*HI and *Xho*I (419–805). The resulting fragments were digested with *Xba*I and *Bam*HI (1–276) or *Bam*HI and *Xho*I (419–805), and subcloned into *Xba*I-*Xho*I sites of pBluescript II KS$^+$ to give CA-mAhR/pBS.

pMSCV retroviral vector was a kind gift of Dr. A. Kume (Jichi Medical School, Tochigi, Japan). CA-mAhR/pBS or wt-mAhR/pcDNA was digested with *Xba*I and *Xho*I, and then blunt-ended with T4 DNA polymerase. The resulting fragments were ligated to the blunted *Xba*I site of pMSCV to generate wt-mAhR-RV or CA-mAhR-RV.

pBSK-mAhR was constructed by inserting the 2.5-kb *Xho*I-*Xba*I fragment of mAhR cDNA described in Ema et al. (16) into the *Xho*I/*Xba*I sites of pBluescript II SK$^+$.

Luciferase reporter assay

Before transfection, Hepa-1c1c7 cells were seeded in 96-well plates at 0.6×10^4 cells/well, then incubated at 37°C for 24 h. The cells were then transfected with the pMC6.3k-luc plasmid (30 ng/well) using FuGENE 6 transfection reagent (Roche Diagnostics). After 24 h of transfection, cells were treated for 24 h with a variety of compounds at indicated concentrations. Luciferase activity was then measured by using a PicaGene assay system (Wako Pure Chemical Industries).

EMSA

A double-stranded oligonucleotide XRE probe (17) was end-labeled with [γ-^{32}P]ATP (Amersham Bioscience) by T4 polynucleotide kinase (NEB) and purified by using ProbeQuant G-50 microcolumns (Amersham Biosciences). In vitro-translated mouse AhR and Arnt were prepared by the TnT T7 quick-coupled transcription/translation system (Promega), according to the manufacturer's instruction, using pBSK-mAhR and pBSK-mArnt (18), respectively.

An unprogrammed transcription/translation system (9 μl) or in vitro-translated mouse AhR and Arnt (4.5 μl) were mixed with vehicle (1 μl of DMSO) or chemicals and incubated for 2 h at 30°C. The reaction mixtures were combined with 10 μl of 2× binding buffer (200 mM HEPES-KOH (pH 7.9), 1 M KCl, 2 mM EDTA, 60 mM $MgCl_2$, 6% glycerol, 20 mM DTT, 0.2 mg/ml sonicated salmon sperm DNA, and one of the chemicals). After incubation for 20 min at 25°C, the radiolabeled XRE probe (2×10^4 cpm) was added and incubated for 20 min at 25°C. The reaction mixtures were applied onto 4.8% acrylamide gel in 0.5× Tris-borate-EDTA buffer. After the electrophoresis, the gel was processed on a gel dryer and then protein-DNA interaction was visualized and quantified with the BAS-1500 bio-image analyzing system (Fujifilm). The intensities of the bands were expressed as units of photostimulated luminescence (PSL).

Binding assay

Hepatic cytosols were prepared essentially as described previously (19). Mouse hepatoma cells, Hepa 1c1c7, were grown in modified αMEM supplemented with 10% FBS, sodium bicarbonate, and penicillin/streptomycin. The cells were harvested homogenized in HEDG buffer (25 mM HEPES, 1.5 mM EDTA, 1 mM DTT, 10% glycerol, pH 7.6 adjusted). For preparation of cytosols, membranes were removed by a 45 min centrifugation at 100,000 × *g*, and then the supernatant was stored at −70°C until use.

Specific binding of M50354 to AhR was assessed by trapping of the AhR complex using anti-AhR Ab. Briefly, 1 μl of ^{3}H-labeled M50354 (60 μM in ethanol) and a competitor (60 mM in DMSO) were added to 100-μl aliquots of cytosols (2.0 mg/ml), and then incubated for overnight at 4°C. These mixtures were added to 96-well microplates coated with the anti-AhR Ab (10 μg/ml), and incubated for 2 h at 4°C. These microplates were washed three times with HEDG buffer, and the retained radioactivities were measured using a scintillation counter.

Mice

C57BL/6 mice were obtained from Japan SLC. AhR-deficient ($AhR^{-/-}$) mice (20) were backcrossed with the C57BL/6 strain by 10 generations. The deficient mice were maintained as heterozygous mice in our laboratory. Mating $AhR^{+/-}$ males with $AhR^{+/-}$ females generated $AhR^{+/+}$, $AhR^{+/-}$ and $AhR^{-/-}$ mice. In the following experiments, we used the wt ($AhR^{+/+}$) and homozygous mutant mice ($AhR^{-/-}$) of the littermates. The neonates were genotyped by PCR of DNA from the tail. The sense primer for the wt at the 5′ region of the *AhR* gene was 5′-CGCGGGCACCAT GAGCAG-3′. The antisense primer for intron 1 was 5′-GAGACT CAGCTCCTGGATGG-3′. The same 5′ primer was used as for the mutant type, while the antisense primer for the *LacZ* gene was 5′-CGCCGAGT TAACGCCATCAA-3′. All in vivo animal experiments were approved by the Institutional Animal Use Committee of our institute.

Evaluation of Th1/Th2 balance in vivo

Mice were given 10 μg of DNP-*Ascaris* adsorbed with 4 mg of alum i.p. on day 0. The sensitized mice were orally treated from days 0 to 9 with 100 mg/kg M50367 or vehicle alone (0.5% hydroxyl-propyl-methylcellurose (HPMC): 10 ml/kg). On day 10, plasma samples were obtained to measure total plasma IgE levels by the sandwich ELISA method described by Hirano et al. (21). Subsequently, spleens were collected, and homogenized using a glass homogenizer under sterile conditions. Homogenates were centrifuged at 300 × *g* for 7 min at 4°C and cell pellets were resuspended in RPMI 1640 medium. The cell suspensions were filtered through 40 μm pore size nylon sieves to remove large cell aggregates. The isolated splenocytes were washed twice in the modified RPMI 1640 medium (S-Clone SF-B; Sanko Junyaku) and resuspended in S-Clone SF-B. One milliliter containing 5×10^6 cells was seeded onto 48-well plates and cultured in the presence of 10 μg/ml DNP-*Ascaris* for 18 h at 37°C. The culture supernatants were harvested and stored at −80°C until cytokine determination. IL-4, IL-5, and IFN-γ concentrations in the supernatants were measured using a commercial ELISA kit.

Ag-induced cell infiltration to the peritoneal cavity

Mice were given 10 μg of DNP-*Ascaris* i.p. on day 0. This injection was repeated on day 7, and the sensitized mice were orally given 100 mg/kg/day M50367 or vehicle alone (0.5% HPMC, 10 ml/kg/day) from days 0 to9. On day 10, the peritoneal cells were harvested by lavage (3 ml of saline containing 1% EDTA), and the total cell number was counted with a hemocytometer (Sysmex).

Naive Th cell preparation and evaluation of Th1/Th2 balance in vitro

Naive CD4$^+$CD62L$^+$ Th cells were prepared from murine spleens as described (22, 23). Briefly, splenocytes were treated with FITC-conjugated anti-CD4 mAb (GK1.5) and microbead-conjugated anti-FITC Ab, and then the microbead-labeled CD4$^+$ Th cells were separated by MACS. After washing, the microbeads were cleaved enzymatically. CD4$^+$CD62L$^+$ Th cells were then isolated using microbead-conjugated anti-CD62L mAb (MEL-14) using the MACS system. The obtained cells were confirmed to be >95% pure CD4$^+$CD62L$^+$ Th cells by flow cytometry.

The naive Th cells were seeded at 0.25×10^6 cells/ml in the plates containing immobilized anti-CD3 mAb (5 μg/ml). These cells were cultured in RPMI 1640 medium containing 10 mM HEPES (pH 7.4), 10%

FBS, 100 U/ml penicillin, 0.1 mg/ml streptomycin, 50 μM 2-ME, and 1 μg/ml anti-CD28 mAb. Three days after the stimulation, a portion of the culture supernatant was sampled for ELISA, and then the cells were expanded 3-fold in a fresh medium. On day 6, Th cells were stimulated again with immobilized anti-CD3 mAb for 6 h in the presence of 4 μM monensin to prevent the release of cytokines. After being stained with FITC-conjugated anti-CD4 mAb (GK1.5/4), the restimulated Th cells were sequentially permeabilized and fixed with Cytofix/CytoPerm (BD Pharmingen). Intracellular cytokines were detected with allophycocyanin-conjugated anti-IFN-γ (XMG1.2) and PE-conjugated anti-IL-4 (11B11) Abs, as described by the manufacturer's protocol (BD Pharmingen). Flow cytometric analysis was performed using FACSCalibur and CellQuest software (BD Biosciences). The axes were set such that the total positive population of isotype control may be below 1%.

Retroviral transduction

A retroviral packaging cell line, phenix (eco) cell, was transfected with CA-mAhR-RV or wt-mAhR-RV using FuGENE6. After 4 or 5 days of culture, PT67 cells (24) were infected with the supernatants from transfected phenix cells. Bright GFP-positive PT67 cells were selected for the preparation of high titer retroviral production cells.

Naive $CD4^+CD62L^+$ Th cells were activated as described above and infected on days 2 and 4 with solutions containing viral supernatant and 6 μg/ml polybrene (Sigma-Aldrich) at a 1:1 volume ratio. The cells were grown for 5 days after the primary activation, and intracellular cytokine staining was performed as described above.

Western blot analysis of AhR

Naive $CD4^+$ Th cells were activated as described above. At 24, 48, and 72 h after activation, the cells were harvested, washed with PBS^-, and lysed in SDS sample buffer (Daiichi Pure Chemicals) for 10 min at 99°C. The protein concentrations were measured by DC Protein Assay (Bio-Rad). Total proteins (10 μg) were separated by 7.5% SDS-PAGE, and then transferred to Fluorotrans W membrane filters (Pall Gelman Laboratory). The membrane filters were incubated with a rabbit polyclonal anti-AhR Ab (BIOMOL) or a rabbit polyclonal anti-Zap70 Ab (Santa Cruz Biotechnology), followed by detection with secondary peroxidase-conjugated anti-rabbit immunoglobulins (DakoCytomation). Signals on the filters were visualized with ECL plus Western blot detection reagent (Amersham Bioscience).

Quantitative transcript analysis

Total RNA was prepared from cultured cells using TRIzol reagent. Quantitative real-time PCR assay was performed using gene-specific primers and SYBR Green RT-PCR Reagent or TaqMan One-step RT-PCR Master Mix Reagent (Applied Biosystems) on a 7000 Sequence Detector (Applied Biosystems). The following pairs of primers and TaqMan probe were used for the RT-PCR assay: *GATA-3* in TaqMan RT-PCR, forward 5′-CAGAACCGGCCCCTTATCA-3′, reverse 5′-CAGGATGTCCCTGCTCTCCTT-3′, and TaqMan probe, 5′-6FAM-TGGCCCCAGCATGCGACCTC-TAMRA-3′; *T-bet*, in SYBR Green RT-PCR, forward 5′-TGCCAGGGAACCGCTTATAT-3′ and reverse 5′-GTTGGAAGCCCCCTTGTTGT-3′. c-*maf*, in SYBR Green RT-PCR, forward 5′-AAGGAGGAGGTGATCCGACT-3′ and reverse 5′-TCTCCTGCTTGAGGTGGTCT-3′. Results were normalized to expression of *β-actin*: forward 5′-GCTCTGGCTCCTAGCACCAT-3′, reverse 5′-GTGGACAGTGAGGCCAGGAT-3′, and TaqMan Probe, 5′-6FAM-TCAAGATCATTGCTCCTCCTGAGCGC-TAMRA-3′. The means ± SD of triplicate determinations are shown.

Statistical analysis

Results were evaluated by Dunnett's procedure for multiple comparisons or Student's *t* test using STAT LIGHT 1997 (Yukms). A difference among groups was considered to be significant when $p < 0.05$.

Results

Binding of M50354 to AhR and enhancement of CYP1A1 promoter activity

As oral administration of M50354 or M50367 induced CYP1A1 expression in mouse liver, we hypothesized that M50354 was an AhR ligand. To confirm this assumption, we examined the in vitro effect of M50354 on CYP1A1 induction, a common property of AhR agonists, in mouse hepatocytes. Hepa1c1c7 cells transiently transfected with pMC6.3k-luc were treated with a variety of concentrations of either M50354 or control compounds for 24 h. We then determined the expression levels of the inducible reporter gene. We observed that M50354 was a relatively weak inducer of CYP1A1, with an EC_{50} greater than 3×10^{-4} M (Fig. 2*A*). Due to a low solubility, we could not test the induction activities of M50354 at concentrations >300 μM. The EC_{50} values for the reference compounds βNF and αNF were estimated to be $\sim 3 \times 10^{-7}$ M and $\sim 1 \times 10^{-5}$ M, which were 3 and 2 orders of magnitude less than that of M50354, respectively. In contrast, resveratrol (25), a control AhR antagonist, had no effect on *CYP1A1* promoter activity at any of the concentrations tested.

To examine whether the addition of M50354 transformed AhR into an active form allowing the interaction with the XRE enhancer sequence, we performed EMSA. In vitro-translated mouse AhR and Arnt were mixed with the radiolabeled XRE probe and several concentrations of M50354. Addition of M50354 induced the formation of an AhR/Arnt/XRE complex in a dose-dependent manner at concentrations exceeding 10 μM (359 PSL at 10 μM, 1204 PSL at 30 μM, and 3601 PSL at 100 μM) (Fig. 2*B*). This result correlates with the induction activity of M50354 in luciferase assays. The reference compounds, 3MC and βNF, also promoted the interaction of AhR/Arnt complex with the XRE at 1 μM (3005 PSL at 1 μM 3MC, 1985 PSL at 0.3 μM βNF, and 2570 PSL at 1 μM βNF); these shifted bands disappeared with competition from excess unlabeled XRE probe. The ability of M50354 to form an AhR/Arnt/XRE complex was relatively weak, which is consistent with its ability to induce *CYP1A1* expression.

To investigate whether M50354 binds AhR, Hepa-1c1c7 cytosol was mixed with 0.6 μM [^{3}H]M50354, then incubated in 96-well plates with an immobilized anti-AhR Ab. After washing, the retained radioactivity was measured. Higher levels of radioactivity were detected in plates with immobilized anti-AhR Ab; this radioactivity could be abolished by the addition of excess competitor, such as unlabeled M50354, αNF, βNF, or 3MC (Fig. 2*C*). This result clearly demonstrated that M50354 specifically binds the AhR protein in a manner similar to other representative AhR ligands.

These results indicate that AhR was activated by M50354 binding. An enhancement of *CYP1A1* promoter activity followed this activation, although this enhancement was not as potent as that induced by αNF, a known partial agonist.

Requirement of AhR for the antiallergic effects of M50367 in vivo

To examine the requirement of AhR in the antiallergic effects mediated by M50367, we administered M50367 to $AhR^{-/-}$ mice.

We first investigated the effects of M50367 on plasma IgE levels in Ag-sensitized mice. $AhR^{-/-}$ and wt mice were sensitized by an i.p. injection of 10 μg of DNP-*Ascaris*/Almu on day 0. Sensitized mice were then treated orally with M50367 (100 mg/kg, daily) for 10 days, beginning on day 0. Orally administered M50367 inhibited IgE production with an EC_{50} value of 1–3 mg/kg (12). Despite the efficacy of low concentrations in this model, however, we used a dosage of 100 mg/kg/day to make the effects of M50367 in $AhR^{-/-}$ mice clear.

Irrespective of AhR genotype, plasma IgE levels in sensitized mice were elevated to levels ~2-fold higher than those observed in nonsensitized mice (Fig. 3*A*). Although the administration of M50367 to wt mice lowered the plasma IgE levels significantly (from 423 ng/ml to 67 ng/ml, $p < 0.01$), this suppression was not observed in $AhR^{-/-}$ mice. The Ag-sensitized $AhR^{-/-}$ mice exhibited 2.5-fold higher serum IgE levels than the wt animals (Fig. 3*A*), although the underlying mechanism remains unclear.

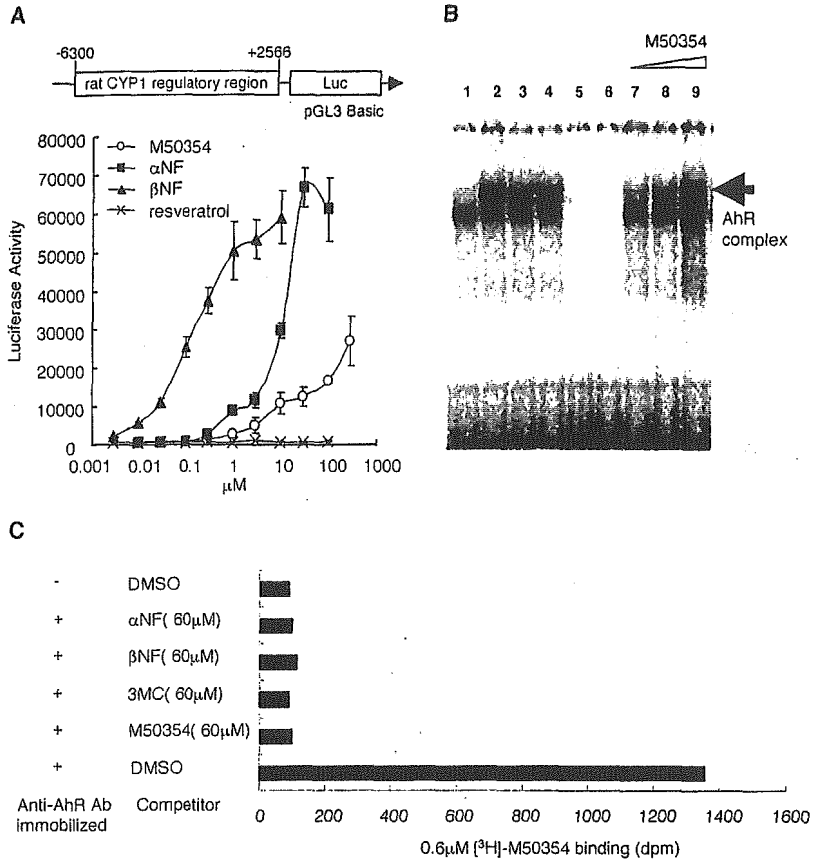

FIGURE 2. M50354 binds to AhR to enhance CYP1A1 promoter activity. *A*, Before transfection, Hepa-1c1c7 cells were seeded in 96-well plates at 0.6×10^4 cells/well, then incubated at 37°C for 24 h. The cells were then transfected with the pMC6.3k-luc plasmid (30 ng/well), the rat CYP1A1 promoter region (−6300 to +2566) ligated with the pGL3 Basic vector, using FuGENE 6 transfection reagent. Twenty-four hours after transfection, cells were treated for 24 h with a variety of compounds at the indicated concentrations. Luciferase activity was then measured using a PicaGene assay system. The means ± SD of quadruplicate determinations are shown. M50354 (○), βNF (▲), αNF (■), resveratrol (x). Data are representative of four independent experiments. *B*, In vitro-translated mouse AhR and Arnt were mixed with either vehicle (1 μl of DMSO) or the indicated chemicals, then incubated for 2 h at 30°C. We then performed EMSA with radiolabeled XRE probe (2×10^4 cpm). *Lanes*: *1*, DMSO control; *2*, 1 μM 3MC treatment; *3*, 0.3 μM βNF treatment; *4*, 1 μM βNF treatment; *5–6*, 1 μM βNF in the presence of a 30- or 100-fold excess of unlabeled XRE probe, respectively; *7–9*, 10, 30, and 100 μM M50354 treatment, respectively. *C*, Cytosols prepared from Hepa-1c1c7 cells were incubated with 0.6 mM [^{3}H]M50354 (37kBq) and competitor (100-fold excess) overnight at 4°C. Samples were added to anti-AhR Ab-coated 96-well plates and incubated for 2 h at 4°C. After washing with PBS$^-$, the retained radioactivity was measured by scintillation.

We then investigated the effects of M50367 on the increases in peritoneal cells induced by repeated Ag sensitization. AhR$^{-/-}$ and wt mice were sensitized twice by i.p. injection of 10 μg of *Ascaris* extract on days 0 and 7. Mice were given M50367 orally (100 mg/kg, daily) for 10 days beginning on day 0, after which the number of peritoneal exudate cells was counted. Although administration of M50367 significantly suppressed the total number of peritoneal exudate cells in the wt mice (from 13.8×10^6 cells to 7.9×10^6 cells, $p < 0.05$), no suppression was observed in *AhR*$^{-/-}$ mice. Ag-sensitized *AhR*$^{-/-}$ mice exhibited a small, but significant, increase in the number of peritoneal exudate cells from the levels observed in their wt counterparts (Fig. 3*B*). This increase in cell number may be related to the elevated serum IgE levels in *AhR*$^{-/-}$ mice.

To evaluate the effects of M50367 on Th1/Th2 balance, we measured cytokine production by ex vivo restimulated splenocytes. In wt splenocytes, the enhanced levels of IL-5 induced by DNP-*Ascaris* sensitization were reduced by treatment with M50367 (from 332 pg/ml to 107 pg/ml, $p < 0.01$), while IFN-γ production was enhanced by M50367 treatment (from 334 pg/ml to 3310 pg/ml, $p < 0.01$) (Fig. 3, *C* and *D*). This result indicated that M50367 administration skewed the Th1/Th2 balance toward Th1 dominance in wt mice. In contrast, M50367 had no effect on either IL-5 or IFN-γ production in *AhR*$^{-/-}$ mice. Interestingly, sensitized *AhR*$^{-/-}$ mice exhibited 3-fold higher IL-5 levels than wt animals treated in a similar manner (Fig. 3, *C* and *D*). Even higher increases in IFN-γ production were observed in sensitized *AhR*$^{-/-}$ mice than those seen in wt animals.

The results of these in vivo experiments indicate that AhR is responsible for the antiallergic and modulatory effects of M50367 on the Th1/Th2 balance.

Modulation effects of M50354 on in vitro Th1/Th2 differentiation from naive Th cells

The addition of M50354 suppressed IL-4 production by naive Th cells and modulated the naive Th cell differentiation into Th1/Th2 cells toward Th1 dominance (13).

Naive Th cells isolated from *AhR*$^{-/-}$ or wt mice were stimulated with anti-CD3 and anti-CD28 mAbs, and then incubated for 6 days in the presence or absence of M50354. We measured the levels of IL-4 and IFN-γ in culture medium by ELISA on day 3 to evaluate the effects of M50354 on early cytokine production, and conducted intracellular cytokine staining on 6 days after treatment to determine the proportions of differentiated Th1/Th2 cells. Addition of M50354 significantly suppressed IL-4 production (1.1–0.4 ng/ml) in wt mice (Fig. 4*A*). M50354 also significantly reduced the population of Th2 cells from 16.4 to 4.5% in these animals (Fig. 4*B*). In *AhR*$^{-/-}$ mice, however, neither IL-4 production nor the proportion of Th2 cells were altered by the addition of M50354 (Fig. 4). AhR-deficient mice exhibited 2- to 3-fold higher levels of both IL-4 and IFN-γ than those seen in wt mice (Fig. 4*A*), a phenotype that is likely associated with enhanced IgE production.

The results of these in vitro experiments indicated that the modulatory effects of M50354 on Th1/Th2 differentiation were mediated by AhR signaling and AhR is likely involved in regulation of the differentiation of naive Th cells into Th1/Th2 cells.

Involvement of AhR signaling in the modulation of Th1/Th2 differentiation

To investigate the role of AhR in the differentiation of naive Th cells, we investigated the expression of AhR throughout the course of Th cell differentiation. Naive Th cells prepared from C57BL/6 mice were stimulated with anti-CD3 and anti-CD28 mAbs. After

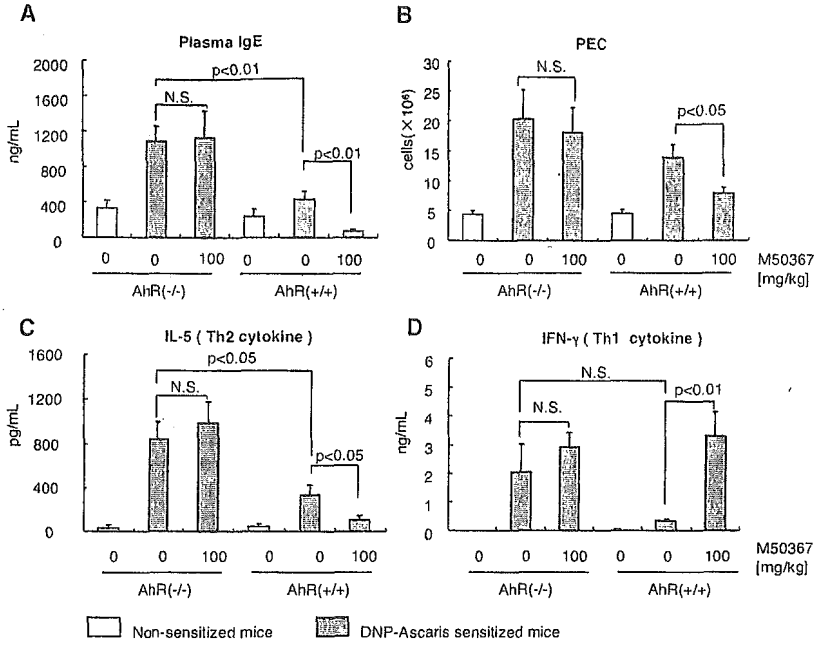

FIGURE 3. Effects of M50367 in in vivo allergic models using $AhR^{-/-}$ and wt mice sensitized with DNP-*Ascaris*. *A*, $AhR^{-/-}$ and wt mice sensitized with 10 μg of DNP-*Ascaris* were given 100 mg/kg M50367 orally. Ten days later, we assessed the IgE concentrations present in plasma samples collected on day 10 by mouse IgE ELISA. *B*, Mice were given 10 μg of DNP-*Ascaris* on day 0. This injection was repeated on day 7; the sensitized mice were treated orally from days 0 to 9 with 100 mg/kg M50367. On day 10, we measured the total number of peritoneal cells collected. *C* and *D*. $AhR^{-/-}$ and wt mice sensitized with 10 μg of DNP-*Ascaris* were given 100 mg/kg M50367 orally for 10 days. On day 10, isolated splenocytes were cultured at 5×10^6 cells/ml in the presence of 10 μg/ml DNP-*Ascaris* in the absence of M50367 for 18 h. We then estimated the concentrations of cytokines present in the supernatants by ELISA. Values are expressed as the means ± SEM of eight animals. $p < 0.05$; $p < 0.01$, calculated by the Student t comparison test.

harvesting the cells at various time points after stimulation, cell lysates were prepared for immunoblot analysis. AhR expression was strongly induced at the earliest time point, and then gradually decreased over the next 72 h (Fig. 5).

To confirm the modulation of Th1/Th2 differentiation by activated AhR, we investigated the effects of a CA-AhR on naive Th cells. Deletion of the ligand-binding domain (PAS B domain) converts AhR into a constitutively active molecule, even in the absence of ligand (15). The CA-AhR and wt-AhR expression vectors were constructed as described in *Materials and Methods* (Fig. 6*A*). After stimulation with anti-CD3 and anti-CD28 mAbs, naive Th cells from $AhR^{-/-}$ mice were infected with a retrovirus encoding wt-AhR or CA-AhR. Cells were cultured in the presence of exogenous IL-4 (10 ng/ml), and then the populations of Th1 and Th2 cells were assessed on day 6 (Fig. 6*B*). Despite the presence of exogenous IL-4, CA-AhR expression induced significant Th1 polarization (3.6–8.8%) with a concomitant decrease in Th2 differentiation (38.5–16.7%). In contrast, wt-AhR transduction did not significantly affect Th1/Th2 differentiation, indicating that activation of AhR modulates Th1/Th2 differentiation toward Th1 dominance.

We examined the modulatory effects of representative AhR ligands on Th cell differentiation. Naive Th cells isolated from wt C57BL/6 mice were stimulated with anti-CD3 and anti-CD28 mAbs in the presence of one of the following compounds: 3MC and βNF as AhR agonists, αNF as a partial antagonist, and resveratrol as a complete antagonist. We assessed the Th1 and Th2 cell populations by intracellular cytokine staining with flow cytometry on day 6 (Fig. 6*C*). M50354, 3MC, and βNF suppressed Th2 differentiation (from 16.2 to 8.0, 9.5, and 7.6%, respectively) with concomitant increases in Th1 differentiation (from 21.3 to 25.7, 23.6, and 25.1%, respectively), whereas αNF did not affect Th1/Th2 differentiation. Resveratrol treatment increased both the Th1 and Th2 populations, similar to the result observed in the Ag-sensitized $AhR^{-/-}$ mice. This result indicates that immunological responses following AhR antagonist treatment mimic the AhR deficiency status of mice. The estimated IC_{50} value of M50354 (~3 μM), βNF (~3 μM), and αNF (> 10 μM) for the inhibition of IL-4 production (Fig. 6*D*) did not agree with the observed EC_{50} for the induction of CYP1A1 expression (Fig. 2*A*), suggesting that AhR uses different molecular mechanisms in these processes.

Effects of M50354 on expression of genes in Th cell differentiation

Taken together with the result that M50354 treatment and CA-AhR transduction of naive Th cells suppressed Th2 differentiation, even in the presence of excess exogenous IL-4 (Ref. 13 and Fig. 6*B*), we presumed that the effect of AhR on Th1/Th2 differentiation likely occurs through modulation of a signaling component upstream of IL-4 action, such as GATA-3 or c-maf. GATA-3 is a master transcriptional factor controlling the differentiation of Th2 cells; impairment of GATA-3 activity by either antisense RNA or a dominant-negative form of the protein potently suppressed Th2 cytokine production and Th2 cell differentiation (26).

To test our hypothesis, we compared the expression of *GATA-3* in $AhR^{-/-}$ mice with that observed in the wt animals. Naive Th cells from $AhR^{-/-}$ and wt littermate mice were stimulated with anti-CD3 and anti-CD28 mAbs. Using RNAs prepared from these cells 24 h after stimulation, we measured the mRNA levels of *GATA-3* and other transcription factors by quantitative RT-PCR (Fig. 7*A*). *GATA-3* expression in naive Th cells isolated from $AhR^{-/-}$ mice exhibited ~3-fold higher GATA-3 mRNA levels than cells derived from wt mice, while the levels of *IL-4Rα*-chain and *STAT6* mRNA were not affected.

From these observations, we hypothesized that the suppression of *GATA-3* expression by activated AhR modulated Th1/Th2 differentiation. Thus, we examined the effect of M50354 on the time course of *GATA-3* mRNA expression. Naive Th cells isolated from C57BL/6 mice were stimulated with anti-CD3 and anti-CD28 mAbs in the presence or absence of M50354. At various time points after treatment, we used quantitative RT-PCR to measure the mRNA levels of *GATA-3* and other transcription factors within RNA samples prepared from these Th cells (Fig. 7*B*). In the absence of M50354, expression of *GATA-3* mRNA began to increase at 48 h, continuing to increase throughout the course of the experiment until 96 h. In the presence of M50354, however, *GATA-3* mRNA expression was already suppressed at 48 h, remaining low at ~10% of control levels at 96 h. mRNA expression levels of c-*maf* and *T-bet* were similarly increased in either the presence or absence of M50354. IL-4 protein production, quantitated by ELISA, began to increase at 72 h in untreated controls; M50354

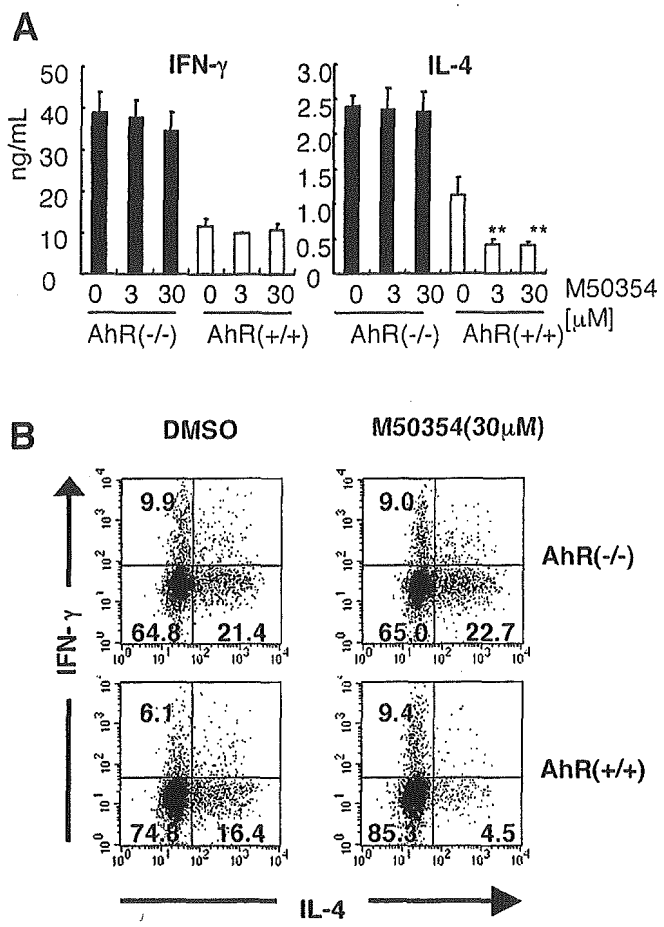

FIGURE 4. Effect of M50354 on the in vitro differentiation of naive Th cells of $AhR^{-/-}$ and wt mice into Th1 and Th2 cells. Naive Th cells prepared from $AhR^{-/-}$ or wt mice were stimulated with immobilized anti-CD3 (5 μg/ml) and anti-CD28 (1 μg/ml) mAbs, then cultured with 3 μm or 30 μM M50354. *A*, On day 3, culture supernatants were harvested; the levels of IL-4 and IFN-γ in these samples were determined by ELISA. Values are expressed as the means ± SD of four independent experiments. **, $p < 0.01$, calculated by Dunnett's procedure for multiple comparisons. *B*, On day 6, cells were restimulated with anti-CD3 mAb in the presence of monensin for 6 h. The proportions of IL-4- and IFN-γ-producing cells were then determined by intracellular cytokine staining, as described in *Materials and Methods*. The percentages of cells present in each quadrant are indicated.

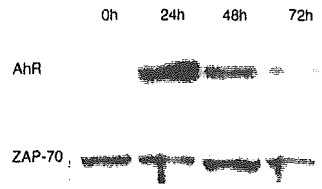

FIGURE 5. Time course of AhR expression during the in vitro differentiation of naive T cells. Naive Th cells prepared from C57BL/6 mice were costimulated with immobilized anti-CD3 (5 μg/ml) and anti-CD28 (1 μg/ml) mAbs. After 24, 48, and 72 h, cells were harvested and analyzed for the expression of AhR proteins by Western blotting using a specific anti-AhR Ab. The image shown is representative of three independent experiments.

treatment reduced these levels to 30% of the observed control levels. These results suggest that M50354 skewed Th1/Th2 differentiation toward Th1 dominance by inhibiting the expression of *GATA-3* in naive Th cells.

Discussion

Recently, there have been an increasing number of reports detailing the various effects of AhR signaling on the immune system, including thymic atrophy and suppression of Ab production, by an AhR ligand, TCDD. Thymic atrophy has been observed in several experimental animal models following exposure to TCDD, reportedly due to the direct effect of TCDD on thymocytes and lymphocyte precursors (27). Furthermore, TCDD exposure suppresses Ag-specific Ab production in mouse models (28, 29). Kerkvliet et al. (30) have also described the marked suppression of CTL responses following TCDD exposure. All of these effects of TCDD have been confirmed to be mediated by AhR signaling by experiments using AhR-deficient mice. These results strongly suggest that AhR is expressed in the T lineage cells, likely functioning in their differentiation and effector function.

The synthetic compound M50367 modulates the Th1/Th2 balance by influencing Th cell differentiation from naive T cells, resulting in the suppression of IgE production and eosinophilic infiltration into sites of inflammation in an in vivo allergy model (12, 13). The modulatory effect of M50354 on Th1/Th2 differentiation from naive Th cells is unique; to our knowledge, there have not been any previous reports detailing the effect of a small molecule, such as this chemical, on the modulation of the Th1/Th2 balance. Therefore, elucidating the mechanism of M50354 action would greatly contribute to our understanding of the mechanisms underlying Th1/Th2 differentiation, potentially facilitating the development of novel antiallergic agents. In this study, we demonstrate that the antiallergic compound M50354 bound and activated AhR, enhancing the expression of a reporter gene driven by the CYP1A1 promoter in transient DNA-transfection assays, gel mobility shift assays, and ligand-binding experiments. We also revealed that M50354 exerted inhibitory effects on Th2 cell differentiation and IgE production in both in vitro and in vivo experiments. As M50354 also suppressed the production of Th2 cytokines, including IL-4 and IL-5, the inhibition of IgE production by M50354 was likely caused by suppression of the differentiation of naive Th cells into Th2 cells, leading to a reduced production of Th2 cytokines. Although the inhibitory effects of this chemical were completely lost in $AhR^{-/-}$ mice, retroviral CA-AhR expression potently inhibited naive Th cell differentiation into Th2 cells in both $AhR^{-/-}$ and wt mice (data not shown), even in the presence of exogenous IL-4. These results indicate that M50354 suppressed Th2 cell differentiation from naive Th cells via activation of AhR signaling, exerting antiallergic effects. 3MC and βNF, representative AhR ligands, also inhibited naive T cell differentiation into Th2 cells and the production of the Th2 cytokines. These findings clearly indicate that AhR signaling regulates the Th1/Th2 balance by influencing Th cell differentiation. The potency of these chemicals to induce *CYP1A1* expression, however, differs from their immunomodulatory activities. M50354 exerted a greater immunomodulatory activity than the examined representative AhR ligands, βNF and 3MC, while the opposite was true for *CYP1A1* induction. Judging from the IC_{50} (~3 μM) for Th2 differentiation and the IC_{50} (> 300 μM) for *CYP1A1* induction, M50354 is specifically more effective in comparison to other AhR ligands at modulating Th cell differentiation than inducing CYP1A1 expression. The conformation of the AhR complex when bound to M50354 may differ from that bound to other AhR ligands. The molecular basis for the differential activities of these AhR ligands will be intriguing to investigate. TCDD, a high affinity AhR ligand, exerts pleiotropic immunosuppressive effects on the production of various Ab isotypes (IgE, IgG1, IgG2, and IgM) (31) and cytokines (IL-2,

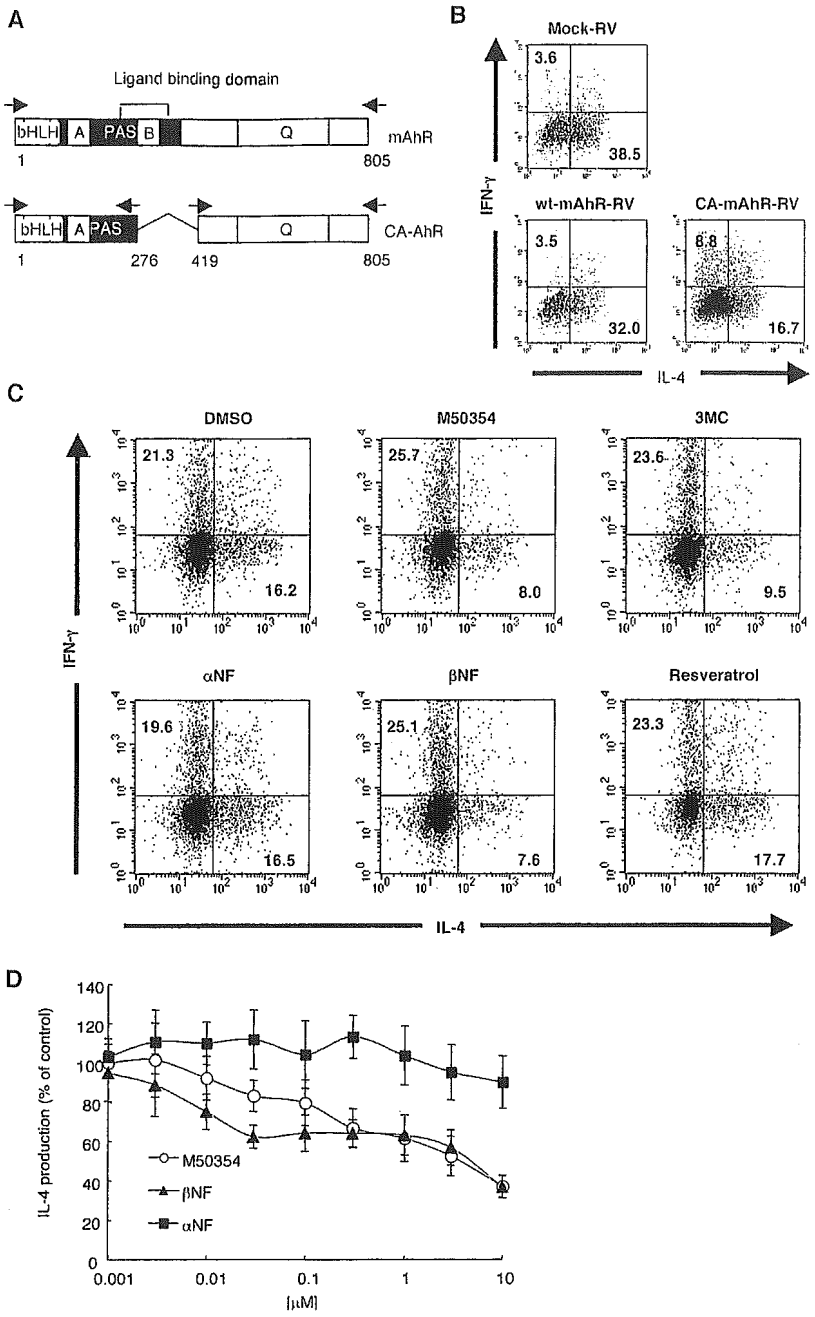

FIGURE 6. Effects of AhR signaling on in vitro Th1/Th2 differentiation. *A*, Schematic representation of the wt AhR and CA-AhR constructs. Q, glutamine rich domain. The positions of the primers used in the plasmid construction are indicated by arrows. *B*, The effects of CA-AhR transduction on Th1/Th2 differentiation. Naive Th cells prepared from $AhR^{-/-}$ mice were stimulated with immobilized anti-CD3 and anti-CD28 mAbs in the presence of IL-4. Cells were then infected with retroviruses encoding the wt AhR, CA-AhR, or control sequences at 24 and 72 h after stimulation. On day 6, cells were harvested and restimulated with anti-CD3 and anti-CD28 mAbs in the presence of monensin. Six hours later, cells were harvested to determine the proportions of IL-4- and IFN-γ-producing cells by intracellular cytokine staining, as described in the *Materials and Methods*. The percentages of cells present in each quadrant are indicated. *C*, Effects of AhR agonists and antagonists on Th1/Th2 differentiation. Naive Th cells prepared from C57BL/6 mice were stimulated with anti-CD3 and anti-CD28 mAbs in the presence of each AhR ligand (3 μM). Six days after stimulation, the cells were collected and restimulated with anti-CD3 and anti-CD28 mAbs in the presence of monensin. Six hours later, cells were harvested to determine the proportions of IL-4- and IFN-γ-producing cells by intracellular cytokine staining. The percentages of the cells present in each quadrant are indicated. *D*, Dose-dependent effect of each chemical on IL-4 production. Naive Th cells prepared from C57BL/6 mice were stimulated with anti-CD3 and anti-CD28 mAbs in the presence of varying concentrations of the indicated chemicals. On day 3, culture supernatants were harvested. The levels of IL-4 were then determined by ELISA. Values are expressed as the means ± SD of four experiments.

IL-4, IL-5, and IL-6). The majority of the effects of TCDD effects, if not all, are thought to be mediated by AhR. In contrast, M50367 did not affect the production of IgG2a, IgM, IL-2, or IL-6; its effects appear to be limited to Th2-mediated immune responses (12). Although M50364 treatment suppressed the expression of *GATA-3*, a key transcription factor for Th2 cell differentiation, it is not known whether activated AhR is directly involved in *GATA-3* expression. As the molecular mechanisms underlying T cell-specific *GATA-3* expression are complex and difficult to investigate (32), we are now investigating the mechanism of *GATA-3* expression inhibition by activated AhR. In the AhR-deficient mice, plasma IgE levels were significantly increased in comparison to those observed in wt mice; the production of both IL-5 and IFN-γ was 2- to 3-fold higher in the primary cultures of $AhR^{-/-}$ Th cells than that seen in wt animals. In AhR-deficient mice, the populations of both Th1 and Th2 cells were increased. Moreover, treatment with resveratrol, an AhR antagonist, enhanced cytokine production in a manner similar that seen in $AhR^{-/-}$ mice. These results indicate that AhR suppresses immune responses under normal conditions; ablation of AhR activity by either gene disruption or antagonist treatment also enhances immune responses. In the first description of AhR-deficient mice, Gonzalez and colleagues (33) reported a decreased accumulation of lymphocytes in the spleen and the lymph nodes, suggesting the requirement for AhR in the development of the immune system. In contrast, Kerkvliet and colleagues (34) reported that AhR-deficient mice generate normal immune responses in Ag-stimulation models. The apparent discrepancies between these results may result from differences in either the mouse stains or the methods used. More extensive analyses using a variety of immunological parameters and analytical methods should be performed to clarify these apparent discrepancies.

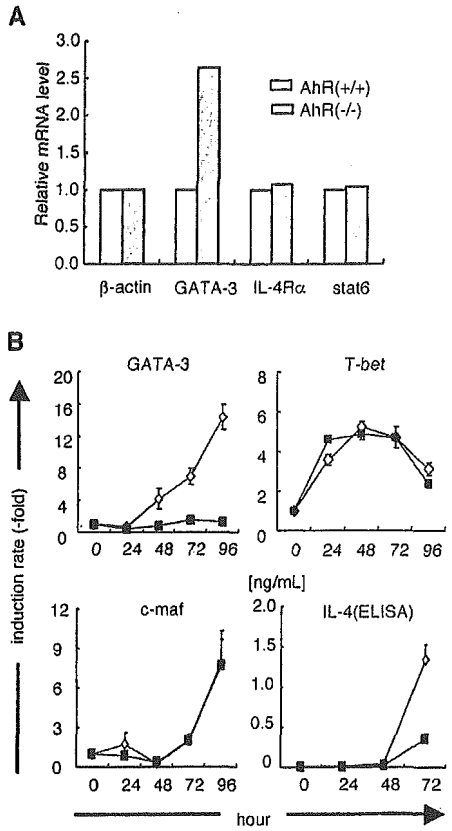

FIGURE 7. Effects of AhR signaling and M50354 treatment on *GATA-3* expression. *A*, Naive Th cells prepared from $AhR^{-/-}$ or wt mice were stimulated with immobilized anti-CD3 (5 μg/ml) and anti-CD28 (1 μg/ml) mAbs. After 24 h, cells were harvested and analyzed for gene expression by quantitative RT-PCR using an ABI7000 analyzer. Data are normalized to the expression levels of each gene in $AhR^{+/+}$ mice. *B*, Naive Th cells prepared from C57BL/6 mice were stimulated with immobilized anti-CD3 (5 μg/ml) and anti-CD28 (1 μg/ml) mAbs in the presence of either vehicle alone (diamonds) or M50354 (squares). After 72 h of culture, cells were expanded 6-fold in fresh medium, then cultured for an additional day. After 24, 48, 72, and 96 h of culture, the harvested cells were analyzed for gene expression by quantitative RT-PCR. Data are normalized to *β-actin* mRNA expression level. The means ± SD of triplicate determinations are shown.

Concerning the role of AhR signaling in the human immune system, Weisglas-Kuperus et al. (35) have reported that perinatal exposure to polychlorinated biphenyls (PCBs) and dioxins is associated with a lower prevalence of allergic diseases in preschool age children. These authors suggested that the lower prevalence is due to the susceptibility to infectious diseases in infants. Taken together with our results, the combined effects of infectious diseases and Th1-dominated conditions caused by exposure to PCBs and dioxins may act synergistically to prevent allergic diseases. Recently, Li et al. (36, 37) have reported the pharmacological actions of MSSM-002, a Chinese herbal formula used as an anti-asthma drug. The effects of MSSM-002 on animal models of allergy are similar to those observed for M50367, exhibiting IgE production inhibition and Th1-dominant differentiation with suppression of *GATA-3* expression. As MSSM-002 is a plant derivative that is abundant in a broad range of flavonoids, also probable AhR ligands, the antiallergic effects of this drug are likely mediated by AhR signaling.

We have demonstrated that M50367 is an AhR ligand of AhR that modulates the Th1/Th2 balance by influencing the differentiation of naive Th cells into Th1 dominance. This effect is probably mediated by down-regulation of *GATA-3* expression, resulting in antiallergic activity. These results suggest that AhR signaling plays a significant role in normal immune responses, making AhR signaling a promising target for chemo therapeutic agents for the treatment of allergic diseases.

Acknowledgments

We thank Yoshitaka Hosaka, Yusuke Shimizu and Tadashi Manabe for their helpful discussion.

Disclosures

The authors have no financial conflict of interest.

References

1. Denis, M., S. Cuthill, A. C. Wikstrom, L. Poellinger, and J. A. Gustafsson. 1988. Association of the dioxin receptor with the M_r 90,000 heat shock protein: a structural kinship with the glucocorticoid receptor. *Biochem. Biophys. Res. Commun.* 155: 801–807.
2. Perdew, G. H. 1988. Association of the Ah receptor with the 90-kDa heat shock protein. *J. Biol. Chem.* 263: 13802–13805.
3. Carver, L. A., J. J. LaPres, S. Jain, E. E. Dunham, and C. A. Bradfield. 1998. Characterization of the Ah receptor-associated protein, ARA9. *J. Biol. Chem.* 273: 33580–33587.
4. Kazlauskas, A., L. Poellinger, and I. Pongratz. 1999. Evidence that the co-chaperone p23 regulates ligand responsiveness of the dioxin (aryl hydrocarbon) receptor. *J. Biol. Chem.* 274: 13519–13524.
5. Fujii-Kuriyama, Y., M. Ema, J. Mimura, and K. Sogawa. 1994. Ah receptor: a novel ligand-activated transcription factor. *Exp. Clin. Immunogenet.* 1: 65–74.
6. Fernandez-Salguero, P. M., D. M. Hilbert, S. Rudikoff, J. M. Ward, and F. J. Gonzalez. 1996. Aryl-hydrocarbon receptor-deficient mice are resistant to 2,3,7,8-tetrachlorodibenzo-*p*-dioxin-induced toxicity. *Toxicol. Appl. Pharmacol.* 140: 173–179.
7. Silkworth, J. B., L. A. Antrim, and G. Sack. 1986. Ah receptor mediated suppression of the antibody response in mice is primarily dependent on the Ah phenotype of lymphoid tissue. *Toxicol. Appl. Pharmacol.* 86: 380–390.
8. Ohtake, F., K. Takeyama, T. Matsumoto, H. Kitagawa, Y. Yamamoto, K. Nohara, C. Tohyama, A. Krust, J. Mimura, P. Chambon, et al. 2003. Modulation of oestrogen receptor signaling by association with the activated dioxin receptor. *Nature* 423: 545–550.
9. Dragan, Y. P., and D. Schrenk. 2000. Animal studies addressing the carcinogenicity of TCDD (or related compounds) with an emphasis on tumour promotion. *Food Addit. Contam.* 17: 289–302.
10. Puga, A., C. R. Tomlinson, and Y. Xia. 2005. Ah receptor signals cross-talk with multiple developmental pathways. *Biochem. Pharmacol.* 69: 199–207.
11. Kerkvliet, N. I. 2002. Recent advances in understanding the mechanisms of TCDD immunotoxicity. *Int. Immunopharmacol.* 2: 277–291.
12. Kato, Y., T. Manabe, Y. Tanaka, and H. Mochizuki. 1999. Effect of an orally active Th1/Th2 balance modulator, M50367, on IgE production, eosinophilia, and airway hyper responsiveness in mice. *J. Immunol.* 162: 7470–7479.
13. Kato, Y., T. Negishi, S. Furusako, K. Mizuguchi, and H. Mochizuki. 2003. An orally active Th1/Th2 balance modulator, M50367, suppresses Th2 differentiation of naive Th cell in vitro. *Cell. Immunol.* 224: 29–37.
14. Fujisawa-Sehara, A., K. Sogawa, C. Nishi, and Y. Fujii-Kuriyama. 1986. Regulatory DNA elements localized remotely upstream from the drug-metabolizing cytochrome P-450c gene. *Nucleic Acids Res.* 14: 1465–1477.
15. McGuire, J., K. Okamoto, M. L. Whitelaw, H. Tanaka, and L. Poellinger. 2001. Definition of a dioxin receptor mutant that is a constitutive activator of transcription: delineation of overlapping repression and ligand binding functions within the PAS domain. *J. Biol. Chem.* 276: 41841–41849.
16. Ema, M., K. Sogawa, N. Watanabe, Y. Chujoh, N. Matsushita, O. Gotoh, Y. Funae, and Y. Fujii-Kuriyama. 1992. cDNA cloning and structure of mouse putative Ah receptor. *Biochem. Biophys. Res. Commun.* 184: 246–253.
17. Matsushita, N., K. Sogawa, M. Ema, A. Yoshida, and Y. Fujii-Kuriyama. 1993. A factor binding to the xenobiotic responsive element (XRE) of *P-450IA1* gene consists of at least two helix-loop-helix proteins, Ah receptor and Arnt. *J. Biol. Chem.* 268: 21002–21006.
18. Numayama-Tsuruta, K., A. Kobayashi, K. Sogawa, and Y. Fujii-Kuriyama. 1997. A point mutation responsible for defective function of the aryl-hydrocarbon-receptor nuclear translocator in mutant Hepa-1c1c7 cells. *Eur. J. Biochem.* 246: 486–495.
19. Zhou, J. G., E. C. Henry, C. M. Palermo, S. D. Dertinger, and T. A. Gasiewicz. 2003. Species-specific transcriptional activity of synthetic flavonoids in guinea pig and mouse cells as a result of differential activation of the aryl hydrocarbon receptor to interact with dioxin-responsive elements. *Mol. Pharmacol.* 63: 915–924.
20. Mimura, J., K. Yamashita, K. Nakamura, M. Morita, T. N. Takagi, K. Nakao, M. Ema, K. Sogawa, M. Yasuda, M. Katsuki, and Y. Fujii-Kuriyama. 1997. Loss of teratogenic response to 2,3,7,8-tetrachlorodibenzo-*p*-dioxin (TCDD) in mice lacking the Ah (dioxin) receptor. *Genes Cells* 2: 645–654.
21. Hirano, T., N. Yamakawa, H. Miyajima, K. Maeda, S. Takaki, A. Ueda, O. Taniguchi, H. Hashimoto, S. Hirose, K. Okumura, and Z. Ovary. 1989. An improved method for the detection of IgE Ab of defined specificity by ELISA using rat anti-IgE mAb. *J. Immunol. Methods* 119: 145–150.

22. Flynn, S., K. M. Toellner, C. Raykundalia, M. Goodall, and P. Lane. 1998. CD4 T cell cytokine differentiation: the B cell activation molecule, OX40 ligand, instructs CD4 T cells to express interleukin 4 and up-regulates expression of the chemokine receptor, Blr-1. *J. Exp. Med.* 188: 297–304
23. Assenmacher, M., M. Lohning, A. Scheffold, A. Richter, S. Miltenyi, J. Schmitz, and A. Radbruch. 1998. Commitment of individual Th1-like lymphocytes to expression of IFN-γ versus IL-4 and IL-10: selective induction of IL-10 by sequential stimulation of naive Th cells with IL-12 and IL-4. *J. Immunol.* 161: 2825–2832.
24. Miller, A. D., and F. Chen. 1996. 1996. Retrovirus packaging cells based on 10A1 murine leukemia virus for production of vectors that use multiple receptors for cell entry. *J. Virol.* 70: 5564–5571.
25. Casper, R. F., M. Quesne, I. M. Rogers, T. Shirota, A. Jolivet, E. Milgrom, and J. F. Savouret. 1999. Resveratrol has antagonist activity on the aryl hydrocarbon receptor: implications for prevention of dioxin toxicity. *Mol. Pharmacol.* 56: 784–790.
26. Zheng, W., and R. A. Flavell. 1997. The transcription factor GATA-3 is necessary and sufficient for Th2 cytokine gene expression in CD4 T cells. *Cell* 89: 587–596
27. Laiosa, M. D., A. Wyman, F. G. Murante, N. C. Fiore, J. E. Staples, T. A. Gasiewicz, and A. E. Silverstone. 2003. Cell proliferation arrest within intrathymic lymphocyte progenitor cells causes thymic atrophy mediated by the aryl hydrocarbon receptor. *J. Immmol.* 171: 4582–4591.
28. Fujimaki, H., K. Nohara, T. Kobayashi, K. Suzuki, K. Eguchi-Kasai, S. Tsukumo, M. Kijima, and C. Tohyama. 2002. Effect of a single oral dose of 2,3,7,8-tetrachlorodibenzo-*p*-dioxin on immune function in male NC/Nga mice. *Toxicol. Sci.* 66: 117–124.
29. Ito, T., K. Inouye, H. Fujimaki, C. Tohyama, and K. Nohara. 2002. Mechanism of TCDD-induced suppression of antibody production: effect on T cell-derived cytokine production in the primary immune reaction of mice. *Toxicol. Sci.* 70: 46–54.
30. Kerkvliet, N. I., D. M. Shepherd, and L. Baecher-Steppan. 2002. T lymphocytes are direct, aryl hydrocarbon receptor (AhR)-dependent targets of 2,3,7,8-tetrachlorodibenzo-*p*-dioxin (TCDD): AhR expression in both $CD4^+$ and $CD8^+$ T cells is necessary for full suppression of a cytotoxic T lymphocyte response by TCDD. *Toxicol. Appl. Pharmacol.* 185: 146–152.
31. Shepherd, D. M., E. A. Dearstyne, and N. I. Kerkvliet. 2000. The effects of TCDD on the activation of ovalbumin (OVA)-specific DO11.10 transgenic $CD4^+$ T cells in adoptively transferred mice. *Toxicol. Sci.* 56: 340–350.
32. George, K. M., M. W. Leonard, M. E. Roth, K. H. Lieuw, D. Kioussis, F. Grosveld, and J. D. Engel. 1994. Embryonic expression and cloning of the murine GATA-3 gene. *Development* 120: 2673–2686.
33. Fernandez-Salguero, P., T. Pineau, D. M. Hilbert, T. McPhail, S. S. Lee, S. Kimura, D. W. Nebert, S. Rudikoff, J. M. Ward, and F. J. Gonzalez. 1995. Immune system impairment and hepatic fibrosis in mice lacking the dioxin-binding Ah receptor. *Science* 268: 722–726.
34. Vorderstrasse, B. A., L. B. Steppan, A. E. Silverstone, and N. I. Kerkvliet. 2001. Aryl hydrocarbon receptor-deficient mice generate normal immune responses to model antigens and are resistant to TCDD-induced immune suppression. *Toxicol. Appl. Pharmacol.* 171: 157–164.
35. Weisglas-Kuperus, N., S. Patandin, G. A. Berbers, T. C. Sas, P. G. Mulder, P. J. Sauer, and H. Hooijkaas. 2000. Immunologic effects of background exposure to polychlorinated biphenyls and dioxins in Dutch preschool children. *Environ. Health Perspect.* 108: 1203–1207.
36. Li, X. M., C. K. Huang, T. F. Zhang, A. A. Teper, K. Srivastava, B. H. Schofield, and H. A. Sampson. 2000. The Chinese herbal medicine formula MSSM-002 suppresses allergic airway hyperreactivity and modulates Th1/Th2 responses in a murine model of allergic asthma. *J. Allergy Clin. Immunol.* 106: 660–668.
37. Srivastava, K., A. A. Teper, T. F. Zhang, S. Li, M. J. Walsh., C. K. Huang, M. Kattan, B. H. Schofield, H. A. Sampson, and X. M. Li. 2004. Immunomodulatory effect of the antiasthma Chinese herbal formula MSSM-002 on Th2 cells. *J. Allergy Clin. Immunol.* 113: 268–276.

MOLECULAR AND CELLULAR BIOLOGY, Nov. 2005, p. 10040–10051 Vol. 25, No. 22
0270-7306/05/$08.00 0 doi:10.1128/MCB.25.22.10040–10051.2005

Intrinsic Function of the Aryl Hydrocarbon (Dioxin) Receptor as a Key Factor in Female Reproduction

Takashi Baba,[1] Junsei Mimura,[2,4] Naohito Nakamura,[1,4] Nobuhiro Harada,[3] Masayuki Yamamoto,[2] Ken-ichirou Morohashi,[1,4]† and Yoshiaki Fujii-Kuriyama[2,4]*†

Department of Developmental Biology, National Institute for Basic Biology, 5-1 Higashiyama, Myodaiji-cho, Okazaki, Aichi 444-8787, Japan[1]; TARA Center, University of Tsukuba, 1-1-1 Tennoudai, Tsukuba, Ibaraki 305-8577, Japan[2]; Department of Biochemistry, Fujita Health University School of Medicine, 1-98 Dengakugakubo, Kutsukake-cho, Toyoake, Aichi 470-1192, Japan[3]; and Solution Oriented Research for Science and Technology, Japan Science and Technology Agency, 4-1-8 Honcho, Kawaguchi, Saitama 332-0012, Japan[4]

Received 20 May 2005/Returned for modification 2 July 2005/Accepted 3 September 2005

Dioxins exert a variety of adverse effects on organisms, including teratogenesis, immunosuppression, tumor promotion, and estrogenic action. Studies using aryl hydrocarbon receptor (AhR)-deficient mice suggest that the majority of these toxic effects are mediated by the AhR. In spite of the adverse effects mediated by this receptor, the AhR gene is conserved among a number of animal species, ranging from invertebrates to vertebrates. This high degree of conservation strongly suggests that AhR possesses an important physiologic function, and a critical function is also supported by the reduced fertility observed with AhR-null female mice. We demonstrate that AhR plays a crucial role in female reproduction by regulating the expression of ovarian P450 aromatase (*Cyp19*), a key enzyme in estrogen synthesis. As revealed by in vitro reporter gene assay and in vivo chromatin immunoprecipitation assay, AhR cooperates with an orphan nuclear receptor, Ad4BP/SF-1, to activate *Cyp19* gene transcription in ovarian granulosa cells. Administration to female mice of an AhR ligand, DMBA (9,10-dimethyl-1,2-benzanthracene), induced ovarian *Cyp19* gene expression, irrespective of the intrinsic phase of the estrus cycle. In addition to elucidating a physiological function for AhR, our studies also suggest a possible mechanism for the toxic effects of exogenous AhR ligands as endocrine disruptors.

The aryl hydrocarbon receptor (AhR), a member of the growing superfamily of basic helix-loop-helix (bHLH)-PAS transcription factors, functions as an intracellular mediator of xenobiotic signaling pathways (37). AhR was originally discovered to occur in hepatocytes as a transcription factor that binds with high affinity to an environmental contaminant, 2,3,7,8-tetrachlorodibenzo-*p*-dioxin (also referred to as TCDD or dioxin) (49). The molecular properties of AhR as a transcription factor have been elucidated by studies of *CYP1A1* gene expression. Normally, AhR exists in the cytoplasm as part of a complex with Hsp90, XAP2, and p23 (28, 34, 35). Upon binding of xenobiotics, such as TCDD and 3-methylcholanthrene (3MC), the receptor complex translocates into the nucleus, where AhR heterodimerizes with the AhR nuclear translocator (Arnt) (61). Within the nucleus, the AhR/Arnt heterodimer binds to XREs (*x*enobiotic *r*esponsive *e*lements) in the promoters of target genes to activate gene expression. A number of genes encoding drug-metabolizing enzymes, including *CYP1A1* and genes encoding UDP-glucuronosyl transferase and glutathione *S*-transferase, have been identified as targets of AhR (18, 21). Gene disruption studies have also revealed that AhR functions in the toxicological effects of dioxins, such as teratogenesis, immunosuppression, tumor promotion, and estrogenic action (6, 19, 38, 50, 56). Despite promoting these multiple adverse effects, AhR is conserved throughout a number of animal species, from invertebrates to vertebrates (20), suggesting that AhR plays a fundamental role in some physiologic process in addition to mediating the response to xenobiotics.

Ovarian functions are primarily regulated by the hypothalamus-pituitary-gonadal (HPG) axis. Gonadotropin-releasing hormone (GnRH) is discharged from the hypothalamic central nervous system and transported through the portal vascular system to stimulate the gonadotrophs of the anterior pituitary. Subsequently, the anterior pituitary secretes the gonadotropins follicle-stimulating hormone (FSH) and luteinizing hormone (LH) into the venous system. In the ovary, FSH promotes the development of immature follicles, eventually leading to the formation of mature preovulatory follicles. Upon stimulation with LH, the mature follicles rupture, leading to ovulation (52). Through the period of follicular maturation to ovulation, gonadotropins stimulate ovarian steroid synthesis. FSH upregulates expression of the P450 aromatase (*Cyp19*) gene (51), which catalyzes the final step of estrogenesis. Although the genes regulated by estradiol are largely unknown, the involvement of estradiol in folliculogenesis was revealed by the phenotype of *Cyp19* knockout (ArKO) mice (17). Due to impaired synthesis of estradiol, *Cyp19* knockout females displayed severely impaired follicular development, resulting in defective ovulation. Interestingly, ovarian defects similar to those seen with ArKO mice were observed upon simultaneous disruption of the estrogen receptor genes, ER and ER (14).

* Corresponding author. Mailing address: TARA Center, University of Tsukuba, 1-1-1 Tennoudai, Tsukuba, Ibaraki 305-8577, Japan. Phone: 81-29-853-7323. Fax: 81-29-853-7318. E-mail: ykfujii@tara.tsukuba.ac.jp.
† These authors equally contributed to this work.

Our analysis of AhR-deficient mice revealed a phenotype defective in reproduction that was similar, albeit milder, to that seen with ArKO and ER and ER double knockout (ER KO) mice. AhR-deficient female mice were subfertile, resulting from impaired folliculogenesis and ovulation. These ovarian defects were likely due to insufficient synthesis of estradiol, consistent with the observation that the *Cyp19* gene is a novel target gene of AhR within the ovary. While the mechanisms by which AhR induces drug-metabolizing enzyme genes in response to exogenous ligands have been extensively studied, the intrinsic function of AhR has remained unknown. In this report, we have identified an intrinsic function for AhR, in which this receptor adjusts ovarian estradiol concentrations by regulating *Cyp19* gene transcription. Based on this novel function for AhR, we propose a molecular mechanism by which the AhR ligands, such as DMBA (9,10-dimethyl-1,2-benzanthracene) and TCDD, also function as endocrine disruptors.

MATERIALS AND METHODS

Fertility assessment. For 3 months, eight AhR / and AhR / females each were mated with AhR / or AhR / males. The litter size of each pregnancy, average litter size, and total number of pups were determined. To exclude any effect caused by individual differences in male fertility, two female mice (one AhR / and one AhR /) were housed in the same cage (mating cage) with a single male mouse (AhR / or AhR /). Once known to be pregnant, female mice were isolated until they gave birth. The numbers of pups were counted on the day of bearing. Female mice were returned to mating cages the next day. This experiment continued for 3 months.

Determination of estrus cycle. To determine the estrus cycle phase, vaginal smears were collected by rinsing the vagina with phosphate-buffered saline (PBS) at 1700 h. Collected smears were mounted on glass slides and stained with Giemsa solution. When angular cells or nucleated epithelial cells occupied the majority of the smear, we determined that the mice were in proestrus or estrus. When a multitude of leukocytes were observed, animals were in metestrus or diestrus (42). These observations were performed for 21 consecutive days.

Superovulation. The estrus cycle was induced artificially by intraperitoneal injection of 5 U pregnant-mare serum gonadotropin (PMSG) (Teikoku Zouki, Japan) at 1700 h on day 1 of the experiment and 5 U human chorionic gonadotropin (hCG) (Teikoku Zouki, Japan) at 1700 h on day 3. In this superovulation protocol, follicles developed to the preovulatory stage following PMSG treatment, and ovulation was induced by hCG treatment. Experiments attempting to rescue AhR / ovulation required the intraperitoneal injection of -estradiol (water soluble; Sigma) dissolved in PBS at 1700 h on day 2. Ovulated oocytes were collected from the oviduct and quantified on day 4.

Determination of serum LH concentrations. One hundred microliters of a GnRH agonist, buserelin (Sigma), in vehicle (PBS-0.3% bovine serum albumin) or vehicle alone was injected into the skin behind the necks of ovariectomized AhR / and AhR / females as described previously (11, 57). One hour after the injection, mice were anesthetized with diethyl ether. After collection of serum samples, serum LH concentrations were determined by radioimmunoassay (SRL, Inc., Japan).

Determination of hormone concentrations. After subjecting mice to the superovulation protocol, we collected ovaries at three time points during the preovulatory period (48 h after PMSG treatment [PMSG 48 h], hCG 5 h, and hCG 8 h). Each ovary was weighed and then homogenized in diethyl ether to a concentration of 10 mg tissue/100 l methanol. Aliquots (30 l) of the redissolved materials were subjected to liquid chromatography-mass spectrometry (Applied Biotechnology, Inc., Japan) to determine the concentrations of estradiol and testosterone by comparing intensity values with standard curves made by standard hormones.

Immunohistochemistry. To detect LH, frozen sections (10 m) were prepared from paraformaldehyde-fixed pituitaries of AhR / and AhR / mice, embedded in the Tissue-Tek compound (Sakura Finetechnical Co., Ltd., Japan). After being washed in Tris-buffered saline (50 mM Tris-HCl [pH 7.6], 150 mM NaCl) containing 1 mM $CaCl_2$, slides were boiled in 10 mM sodium citrate (pH 6.0) for antigen unmasking (43) and then treated with methanol at 20°C for 30 min. Sections were then incubated with an antibody against the subunit of LH (Biogenesis) overnight at 4°C, washed, and treated with a biotinylated donkey anti-rabbit immunoglobulin G (Jackson ImmunoResearch Laboratories, Inc.) for 3 h at room temperature. After being washed, sections were developed with horseradish peroxidase-conjugated streptavidin (Nichirei, Japan) and visualized with diaminobenzidine (Nichirei, Japan) for 10 min at room temperature.

To detect AhR and Cyp19, we prepared paraffin sections (5 m) from paraformaldehyde-fixed ovaries isolated from AhR / and AhR / females given PMSG and hCG (hCG 5 h). After deparaffinization, sections were treated with proteinase K (20 g/ml) (Sigma) to unmask antigen epitopes and then treated with hydrogen peroxide (0.3% H_2O_2 in methanol). Sections were incubated overnight at 4°C with either anti-AhR (generously provided by R. Pollenz) or anti-Cyp19 (22) antibody, washed, and then incubated with biotinylated donkey anti-rabbit immunoglobulin G for 3 h at room temperature. After being washed, sections were incubated with horseradish peroxidase-conjugated streptavidin and visualized with diaminobenzidine for 4 min at room temperature.

ChIP assay. We performed chromatin immunoprecipitation (ChIP) as previously described (46, 48), with the following modifications. Briefly, to fix the chromatin-protein complexes, ovaries isolated from AhR / and AhR / females treated with PMSG and hCG (hCG 2 h) were punctured with a needle containing Dulbecco's modified Eagle's medium (DMEM)–Ham F-12 medium–1% FBS with 1% formaldehyde immediately after removal. After fixation was stopped in 125 mM glycine, the suspension of ovarian cells was filtered through a 70- m cell strainer (Falcon). The isolated granulosa cells were then resuspended in lysis buffer (50 mM HEPES [pH 7.4], 140 mM NaCl, 1 mM EDTA, 10% glycerol, 0.5% NP-40, 0.25% Triton X-100). Nuclei were recovered by centrifugation at 4°C for 30 min. After dissolution in Tris-EDTA (10 mM Tris-HCl [pH 7.4], 0.1 mM EDTA), nuclei were sonicated to shear genomic DNA to approximately 1-kb fragments. Sheared chromatin-DNA complexes were then subjected to immunoprecipitation with either anti-AhR or anti-Ad4BP antibody (41). DNA was extracted from the precipitates by incubation with proteinase K at 65°C, followed by treatment with phenol-chloroform. Presence of the *Cyp19* promoter region was determined by PCR with the appropriate primer sets, indicated below.

Transfection and luciferase assay. The 5 -flanking regions of the human *CYP19* and mouse *Cyp19* genes were inserted into the pGL3-basic vector (Invitrogen) to generate h*CYP19*-3853Luc and m*Cyp19*-5335Luc, respectively. Human embryonic kidney-derived 293 cells were grown in DMEM (Sigma, St. Louis, Mo.) supplemented with 10% fetal bovine serum (FBS) at 37°C in 5% CO_2. Cells were plated at approximately 15% confluence 1 day before transfection. Transfections were conducted in triplicate in 24-well plates by using Lipofectamine Plus (Gibco BRL, Gaithersburg, Md.), according to the manufacturer's protocol. Each well received 500 ng reporter plasmid, 10 ng of the reference pBOS-LacZ vector, and one of various concentrations (0 to 50 ng) of the expression plasmid encoding either AhR, Arnt, the AhR repressor (AhRR) (36), or Ad4BP/SF-1 (39). Cells were treated for 3 h with lipofection reagent in DMEM without serum and then incubated for 48 h in DMEM-10% FBS with or without 3MC (Wako, Japan). Cells were harvested and subjected to luciferase and -galactosidase assays. All luciferase activities were normalized to the corresponding -galactosidase activities. Values are represented as the means standard deviations (SD) of three independent experiments.

Immunoprecipitation assay. The full-length cDNAs encoding AhR and Ad4BP/SF-1 were inserted into the expression vectors p3 FLAG-CMV-10 (Sigma) and pEGFP-c1 (Clontech) to generate 3 FLAG-AhR and EGFP-Ad4BP, respectively. These plasmids (1 g) were cotransfected into 293 cells with the expression vector encoding Arnt as described above. An enhanced green fluorescent protein (EGFP) expression vector was included in the transfection as a control. Forty-six hours after transfection, 1 M of 3MC was added to stimulate nuclear translocation of AhR. After a 2-h incubation, cells were harvested in lysis buffer (50 mM Tris-HCl [pH 8.0], 300 mM NaCl, 1.5 mM $MgCl_2$, 1 mM EDTA, 1% Triton X-100, 10% glycerol) containing 1 Complete protease inhibitor cocktail (Roche) (30). FLAG-tagged and associated proteins were immunoprecipitated from whole-cell extracts (400 g) by using anti-FLAG M2-agarose affinity gel (Sigma) in immunoprecipitation buffer (50 mM Tris-HCl [pH 8.0], 150 mM NaCl, 1.5 mM $MgCl_2$, 1 mM EDTA, 1% Triton X-100, 10% glycerol) containing 1 Complete protease inhibitor cocktail. Isolated proteins were subjected to immunoblotting with an anti-GFP antibody (MBL, Nagoya, Japan).

PCR conditions. Primer pairs used for semiquantitative reverse transcription-PCR (RT-PCR) were as follows: AhR(fwd), 5 -CGC GGG CAC CAT GAG CAG-3 ; AhR(rev), 5 -CTG TAA CAA GAA CTC TCC-3 ; AhRR(fwd), 5 -GCT TTC TGT CCT GCG CCT C-3 ; AhRR(rev), 5 -GAA GTC CTG CCG GTC ATC C-3 ; Cyp19(fwd), 5 -TCA ATA CCA GGT CCT GGC TA-3 ; Cyp19(rev), 5 -GTA TGC ACT GAT TCA CGT TC-3 ; P450scc(fwd), 5 -CGA ATC GTC CTA AAC CAA GAG-3 ; P450scc(rev), 5 -CAC TGA TGA CCC CTG AGA AAT-3 ; 3 HSD(fwd), 5 -ACT GCA GGA GGT CAG AGC T-3 ;

3 HSD(rev), 5 -GCC AGT AAC ACA CAG AAT ACC-3 ; P450 17 (fwd), 5 -GGG GCA GGC ATA GAG ACA ACT-3 ; P450 17 (rev), 5 -GGG TGT GGG TGT AAT GAG ATG-3 ; P27^{kip1}(fwd), 5 -AAG CGG ATC ACC CCA AGC CT-3 ; P27^{kip1}(rev), 5 -GTT GGC GGT TTT GTT TTG CG-3 ; C/EBP (fwd), 5 -TCT ACT ACG AGC CCG ACT GCC T-3 ; C/EBP (rev), 5 -AGCTTG TCC ACC GTC TTC TT-3 ; GAPDH(fwd) (GAPDH, glyceraldehyde-3-phosphate dehydrogenase), 5 -GGC ATG GCC TTC CGT GTT CCT-3 ; GAPDH(rev), TCC TTG CTG GGG TGG GTG GTC-3 ; -actin(fwd), 5 -ATG GAT GAC GAT ATC GCT-3 ; and -actin(rev), 5 -ATG AGG TAG TCT GTC AGG T-3 . Thermal-cycling conditions were as follows: 28 cycles of 30 s at 94°C, 30 s at 60°C, and 1 min at 72°C for the amplification of AhR, P27^{kip1}, and C/EBP ; 32 cycles of 30 s at 94°C, 30 s at 58°C, and 1 min at 72°C for AhRR; 25 cycles of 30 s at 94°C, 30 s at 60°C, and 1 min at 72°C for Cyp19, P450scc, 3 HSD, and P450 17 ; and 22 cycles of 30 s at 94°C, 30 s at 60°C, and 1 min at 72°C for GAPDH and -actin. Quantitative RT-PCR was performed with a TaqMan gene expression assay (Applied Biosystems) on a 7500 real-time PCR system (Applied Biosystems). Thermal-cycling conditions were 50 cycles of 15 s at 95°C and 1 min at 60°C.

Primer pairs used for ChIP assays were as follows: XRE of Cyp19 (fwd), TGA GAG TGA ACT GCA GGA AG-3 ; XRE of Cyp19 (rev), ACC TCA TGG CTA AGG CAA TG-3 ; Ad4 of Cyp19 (fwd), ATA AGG AGG ATT GCC TCA GC-3 ; Ad4 of Cyp19 (rev), GCT CCT GTC ACT TGG AAG GG-3 ; 2740 2441 of Cyp19 (fwd), GAC TTT GCA TAG AGA CTT GG-3 ; 2740 2441 of Cyp19 (rev), CTG TTT AGT GTT GTC AAT GC-3 ; -actin(fwd), AGG GTG TGA TGG TGG GAA TGG-3 ; and -actin(rev), TGG CTG GGG TGT TGA AGG TCT-3 . Thermal-cycling conditions were 32 cycles of 30 s at 94°C, 30 s at 62°C, and 1 min at 72°C.

RESULTS

Phenotype of AhR / females related to reproduction. The reproductive defects of AhR / females have remained controversial (1). We therefore examined if fertility was impaired in the AhR / females used in this study. To avoid experimental variation due to genetic background, we used AhR knockout (AhR KO) mice backcrossed to C57BL/6J mice for more than eight generations. For 3 months, AhR / and AhR / females were mated with AhR / or AhR / males, and the number of pups delivered was counted. Using eight randomly selected AhR / and AhR / females, the total number of pups delivered by the AhR / females was 213, while those delivered by AhR / females was 57 (Table 1). The average litter size of AhR / females was approximately 40% that of the wild type. None of the AhR / females examined bore a third litter, and one of these mutant animals was unable to deliver pups during the mating period. Although levels of reproductive activity varied among individuals, these results clearly indicated a decreased fertility of AhR / females.

To explore the causes of AhR / subfertility, we histologically examined the reproductive organs. Examination of the organs revealed a reduction of the ratio of ovarian weight to body weight in the AhR / females to 56% of that seen in the wild-type animals (0.055 0.010% for AhR / versus 0.031 0.003% for AhR / , n 3, P 0.05). In contrast, the uterus appeared to be unaffected (0.272 0.030% for AhR / versus 0.294 0.049% for AhR / , n 3) (Fig. 1A and B). Based on histological analyses, the ovaries of AhR / animals developed follicles up to the antral/preovulatory stage in the presence of slightly hypoplastic interstitial cells (Fig. 1C). The corpus luteum, however, was barely detectable in AhR / ovaries. As the corpora lutea develop from postovulatory follicles, this observation implied a failure in a final step of follicular maturation and/or ovulation.

As failures of follicular maturation and ovulation are frequently accompanied by a disordered estrus cycle (29, 58), we then examined if the ovarian estrus cycle proceeds normally in AhR / mice (Fig. 1D). In wild-type and AhR / mice, the estrus cycle progressed regularly, lasting 4 to 5 days. Although we observed considerable individual variation, AhR / females displayed significantly disordered estrus cycles (Fig. 1D), which we classified into three groups. Mice in group I showed a prolonged cycle. In group II, animals exhibited a cycle that was irregularly shortened or prolonged. Unusually prolonged estrus phases were observed for mice classified as group III. Such irregularities were not observed for AhR / or AhR / mice.

As the HPG axis is crucial for progression of the estrus cycle, we examined the tissues of the HPG axis to determine which region is affected in AhR / animals. First, we examined the ability of the ovaries of AhR / mice to respond to gonadotropins. AhR / females aged 3 and 12 weeks were subjected to a standard superovulation protocol, and the numbers of ovulated oocytes in response to gonadotropin stimulation were counted. In AhR / mice, the total number of the ovulated oocytes decreased to approximately one-sixth the level seen for age-matched wild-type females (Table 2). We then examined the production of gonadotropins in the pituitaries of AhR / animals by immunohistochemical analysis using an anti-LH antibody (Fig. 2A). LH-immunoreactive gonadotrophs were present in the anterior lobes of the pituitary glands of both AhR / and AhR / mice. We then investigated the ability of gonadotrophs to secrete LH in response to stimulation with a GnRH agonist, buserelin (des-Gly$_{10}$-[D-Ser{t-Bu}$_6$]-LH-RH ethylamide). To exclude any feedback effects from the ovaries, animals were ovariectomized prior to experimentation. After subcutaneous injection of buserelin into the ovariectomized mice, we determined the serum LH concentrations. Neither the basal nor the buserelin-induced concentrations differed between AhR / and AhR / mice, indicating that the ability of AhR / gonadotrophs to se-

TABLE 1. Distribution of pups by female genotype

Genotype		No. of pups per litter				Total pups[b]
Female	Male	1st	2nd	3rd	Avg[a]	
AhR /	AhR /	8	11	10	9.7	29
		8	11		9.5	19
		10	10		10.0	20
		9	11	9	9.7	29
AhR /	AhR /	11	13	11	11.7	35
		9	10	11	10.0	30
		9	10	10	9.7	29
		11	11		11.0	22
AhR /	AhR /	4	5		4.5	9
		8			8.0	8
		3	5		4.0	8
						0
AhR /	AhR /	2	1		1.5	3
		2	3		2.5	5
		7	3		5.0	10
		10	4		7.0	14

[a] Average litter sizes for all AhR / females and AhR / females were 10.1 and 4.4, respectively.

[b] Total numbers of pups for all AhR / females and AhR / females were 213 and 57, respectively.

A

	total body (g)	ovary (mg)	ovary / body (%)	uterus (mg)	uterus / body (%)
AhR (+/+)	24.9	13.1 (5.6 + 7.5)	0.053	75.4	0.303
AhR (+/+)	23.1	10.6 (5.2 + 5.4)	0.046	56.3	0.244
AhR (+/+)	24.3	16.0 (8.2 + 7.8)	0.066	65.3	0.269
AhR (−/−)	22.0	7.1 (3.3 + 3.8)	0.032	72.9	0.331
AhR (−/−)	24.1	8.0 (3.2 + 4.8)	0.033	57.6	0.239
AhR (−/−)	21.5	5.8 (3.2 + 2.6)	0.027	67.2	0.313

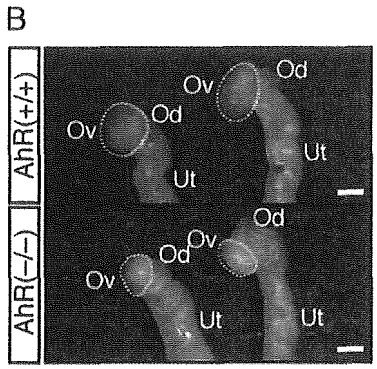

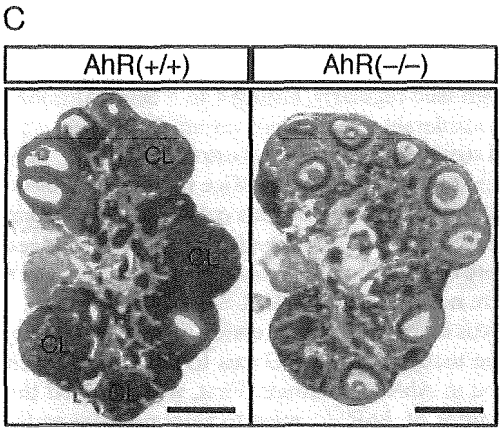

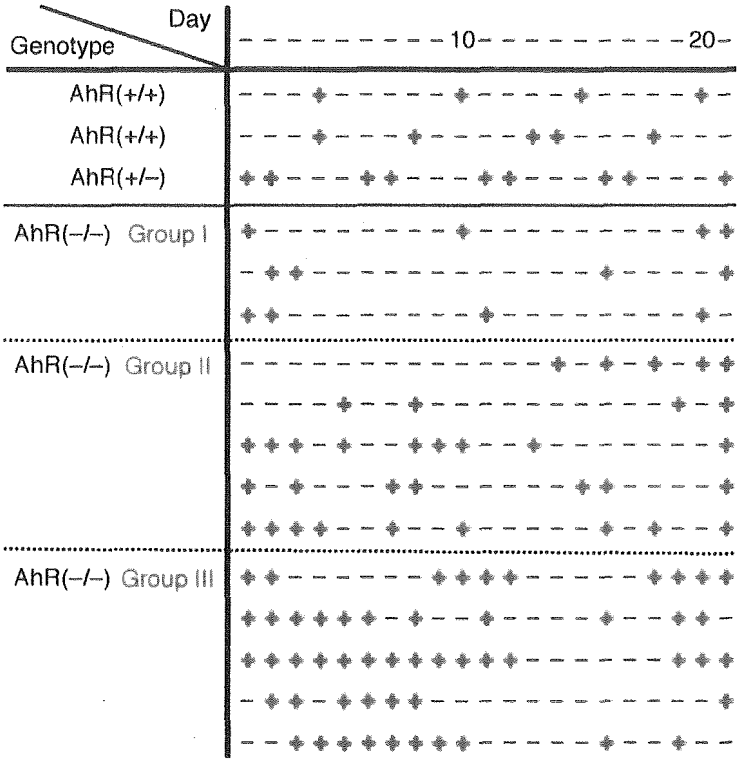

FIG. 1. Estrus cycle and folliculogenesis affected in AhR / ovaries. (A) Ovarian and uterine wet weights of AhR / and AhR / females. The ovaries and uteri isolated from 9-week-old mice were weighed. The ratios of ovarian or uterine wet weight to total body weight are also indicated. Three AhR / and AhR / mice each were examined in this experiment. (B) Morphologies of the reproductive tracts of 9-week-old AhR / and AhR / females. The ovaries are outlined in broken yellow lines. Ov, Od, and Ut indicate the ovary, oviduct, and uterus, respectively. Bar, 1 mm. (C) Histological analysis of the ovaries of AhR / and AhR / mice. Five-micrometer paraffin-embedded sections of AhR / and AhR / ovaries were stained with hematoxylin-eosin. CL indicates the corpus luteum. Bar, 0.5 mm. (D) Disordered estrus cycles in AhR / females. Vaginal smears from AhR / , AhR / , and AhR / female mice were collected for 21 consecutive days and stained with Giemsa solution. , proestrus or estrus; , metestrus or diestrus.

crete gonadotropins in response to upstream signals was not impaired (Fig. 2B). These results strongly suggest that the reduced fertility of AhR / females was due primarily to ovarian defects.

Synthesis of estradiol in AhR / ovaries is insufficient compared with that of the wild type. Estradiol is an essential sex hormone for female reproduction, and serum concentrations increase transiently during the preovulatory stage (54). We measured the concentrations of estradiol in the ovaries at three time points during the preovulatory stage (Fig. 3A). As AhR / females failed to demonstrate normal estrus cycles,

TABLE 2. Numbers of ovulated oocytes according to female genotype

Genotype	Age (wk)	No. of ovulated oocytes (mean SD)	No. of mice
AhR /	3	51.3 2.2	4
	12	25.0 1.0	3
AhR /	3	8.7 8.5	3
	12	4.0 4.6	3

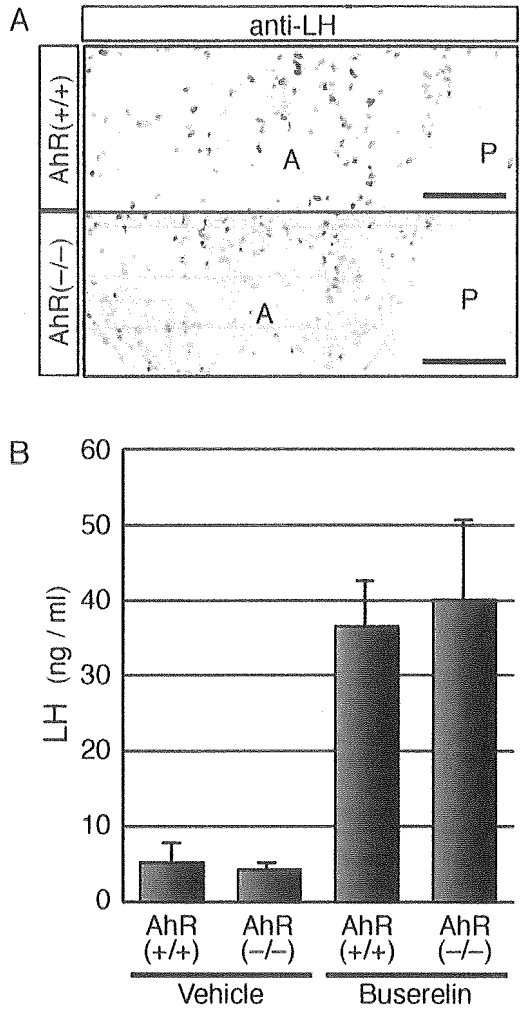

FIG. 2. Functionally normal gonadotropes of AhR / pituitaries. (A) Presence of gonadotrophs in the pituitary anterior lobes of AhR / females. Cryosections of pituitaries isolated from AhR / and AhR / mice were treated with an anti-LH antibody, which should specifically stain pituitary gonadotrophs. A and P represent the anterior and posterior lobes, respectively. Bar, 0.1 mm. (B) Secretion of LH from the gonadotrophs of AhR / pituitaries. A GnRH agonist, buserelin (2 g), or vehicle alone was injected subcutaneously into ovariectomized AhR / and AhR / females. One hour after injection, serum levels of LH were determined. Values are represented as means SD for three to four mice.

we forced the estrus cycle to proceed by gonadotropin stimulation. In AhR / females, the concentrations of intraovary estradiol were decreased to 20 to 30% of the levels seen for wild-type animals at all three time points (Fig. 3B). Testosterone, the precursor of estradiol, was slightly increased in the ovaries of AhR / mice in comparison with the concentrations observed for AhR / females (Fig. 3C). These observations suggest that the decreases in ovarian estradiol are responsible for the reproductive defects of AhR / females. We therefore reasoned that an intraperitoneal injection of estradiol at the appropriate time of the ovulatory cycle would rescue the observed phenotype. AhR / mice were treated at day 2 with estradiol in the superovulation protocol (Fig. 3D), and then released oocytes were quantified. Administration of up to 10 ng estradiol to AhR / mice partially corrected the decrease in the number of ovulated oocytes in a dose-dependent manner. Administration of 20 ng estradiol failed to increase the number of ovulated oocytes further (Fig. 3E). Although these results clearly indicate that insufficient estradiol at least contributes to AhR / subfertility, either the timing or the site of estradiol administration may not have been optimal for full recovery of fertility. Additional factors may also be affected with AhR / mice, influencing the reproduction process.

AhR is indispensable for proper expression of the *Cyp19* gene in the ovary. As AhR functions as a transcription factor, the above observations suggested that this receptor is involved in the transcriptional regulation of steroidogenic genes. The expression pattern of AhR during folliculogenesis, however, is largely unknown. We therefore examined AhR expression throughout an artificially produced estrus cycle in wild-type mice (Fig. 4A). AhR mRNA was expressed throughout the preovulatory period. AhRR, a target of AhR transcriptional regulation, represses AhR function (2, 36). Interestingly, the expression of AhRR was upregulated at 6 and 7 h after hCG injection (Fig. 4B), suggesting that, while AhR becomes functionally active after treatment with PMSG, its activity thereafter is repressed by the action of AhRR. We therefore examined the expression of the *Cyp19* gene, whose product is essential for estradiol production, during folliculogenesis. *Cyp19* gene expression was activated 48 h after PMSG treatment and downregulated gradually after hCG treatment. This downregulation appeared to coincide with the induction of AhRR expression.

We then compared the expression levels of other steroidogenic enzymes within the ovaries of wild-type and AhR / mice at 4 and 7 h after hCG treatment (Fig. 4C). We did not observe any alteration in expression of mRNAs encoding steroidogenic Cyp11A (P450scc), 3 HSD, and Cyp17 (P450 17 , 17 -hydroxylase) between wild-type and knockout animals at the two time points examined. While Cyp19 mRNA was potently upregulated in wild-type ovaries during the final maturation stage of folliculogenesis induced by hormone treatment (Fig. 4B), expression of this gene was markedly reduced in AhR / ovaries, even at 4 h after hCG treatment. Quantitative RT-PCR demonstrated that the expression of Cyp19 in AhR / females was reduced by greater than 90% from that of wild-type animals 4 h after hCG treatment (Fig. 4D), indicating that Cyp19 mRNA expression was not upregulated in AhR / ovaries during hormone treatment. There were no detectable differences between the wild-type and AhR knockout mice in the expression of either $p27^{kip1}$ or C/EBP , both of which are involved in ovulation (16, 29, 47, 58). As expected, there was no expression of AhRR mRNA in AhR / ovaries at 7 h after hCG treatment. To determine if Cyp19 protein levels were also altered in AhR / ovaries, we prepared whole-tissue extracts from hormone-treated ovaries (hCG 5 h) and subjected these samples to Western blot analysis with an anti-Cyp19 antibody. In agreement with the results of our mRNA expression analysis, we detected decreased levels of Cyp19 protein in the ovaries of AhR / mice (Fig. 4E). Consistent with previous reports (53, 62), immunohistochemical staining with anti-AhR and anti-Cyp19 antibodies demonstrated coexpression of AhR and Cyp19 in the granulosa cells of antral follicles (Fig. 4F). We also confirmed by immunohis-

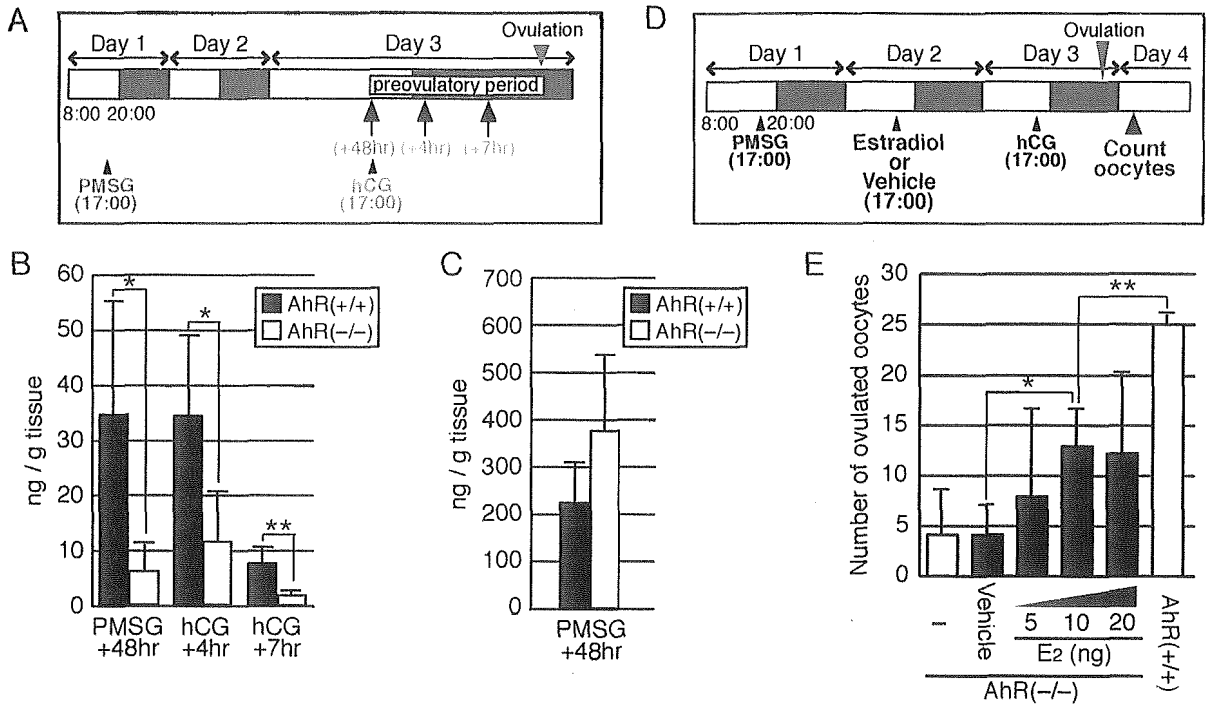

FIG. 3. Concentrations of intraovarian steroids in AhR / females and the rescue of ovulation by estradiol treatment. (A) Schematic representation of the experimental procedure used to determine intraovarian steroid concentrations during the preovulatory period. (B) Intraovarian estradiol concentrations in AhR / and AhR / females. The ovaries of at least three AhR / and three AhR / female mice were collected at the times indicated in panel A. Estradiol concentrations were then determined by liquid chromatography-mass spectrometry analysis. , P 0.10; , P 0.05. (C) Intraovarian testosterone concentrations were determined as described for panel B. (D) Schematic representation of the experimental estradiol administration procedure used to rescue the ovulation of AhR / mice. Mice treated with PMSG at day 1 were divided into two groups. One group was treated with various quantities of estradiol, while the other group was given vehicle alone on day 2. The mice from both groups were treated with hCG on day 3, and ovulation was assessed at day 4. (E) Effects of estradiol administration on ovulation in AhR / females. After the treatment of AhR / and AhR / females with PMSG and hCG, the oocytes released by ovulation were counted (open bars). AhR / females were also given an intraperitoneal injection of 5 to 20 ng 17 -estradiol (E2) or vehicle alone (filled bars) as described for panel D prior to counting the ovulated oocytes. , P 0.025; , P 0.005.

tochemistry that Cyp19 protein levels were diminished in the granulosa cells of AhR / ovaries (Fig. 4F).

AhR directly activates *Cyp19* gene transcription in cooperation with an orphan nuclear receptor, Ad4BP/SF-1. As the previously described results strongly suggest the involvement of AhR in *Cyp19* expression, we examined the mechanism by which AhR regulated *Cyp19* gene transcription. The *Cyp19* gene has multiple tissue-specific first exons (23, 33, 55). In the ovary, this gene is transcribed from exon PII (Ex 1d) in a mechanism involving the orphan nuclear receptor Ad4BP/SF-1 (8, 32, 40, 45). The binding site for Ad4BP/SF-1 is conserved within the 5 upstream regions of the human and mouse genes. We also determined that the human *CYP19* and mouse *Cyp19* genes have an AhR/Arnt-binding sequence (XRE) 3,756 and 5,058 bp upstream of the ovary-specific first exon, respectively (Fig. 5A and B). We therefore transiently transfected the expression vectors of AhR, Arnt, and Ad4BP/SF-1 into cultured cells to investigate the promoter function of the *CYP19/Cyp19* genes. While Ad4BP/SF-1 clearly activated *CYP19/Cyp19* gene transcription, cotransfection of AhR and Arnt resulted in only weak activation. Simultaneous expression of AhR/Arnt with Ad4BP/SF-1, however, synergistically activated the Cyp19 promoter (Fig. 5C and D). Subsequent expression of AhRR suppressed the transcription activation induced by AhR (Fig. 5C and D).

The observed synergistic activation of the *CYP19/Cyp19* promoter by AhR/Arnt and Ad4BP/SF-1 implied a physical interaction between these proteins. To verify this interaction, we cotransfected expression vectors encoding 3 FLAG-AhR, Arnt, and EGFP-Ad4BP/SF-1 and then attempted to coimmunoprecipitate these components by using an anti-FLAG antibody. EGFP-Ad4BP/SF-1, but not EGFP, was coimmunoprecipitated with FLAG-AhR (Fig. 6A), indicating a potential physical interaction between AhR/Arnt and Ad4BP/SF-1. To investigate if AhR binds to the XRE within the promoter of *Cyp19* in vivo, we performed a ChIP assay using chromatin isolated from the granulosa cells of gonadotropin-treated ovaries (Fig. 6B). PCR analysis of the immunoprecipitates isolated using an anti-AhR antibody (Fig. 6B) revealed that the XRE of the *Cyp19* gene was associated with AhR in samples derived from wild-type mice but not AhR / mice (Fig. 6C). This result clearly indicates that AhR was recruited to the *Cyp19* promoter in vivo. As the *Cyp19* gene is synergistically activated by AhR/Arnt and Ad4BP/SF-1, we assumed that AhR, Arnt, and Ad4BP/SF-1 physically interact on the *Cyp19* promoter. We next examined whether anti-AhR antibodies precipitate

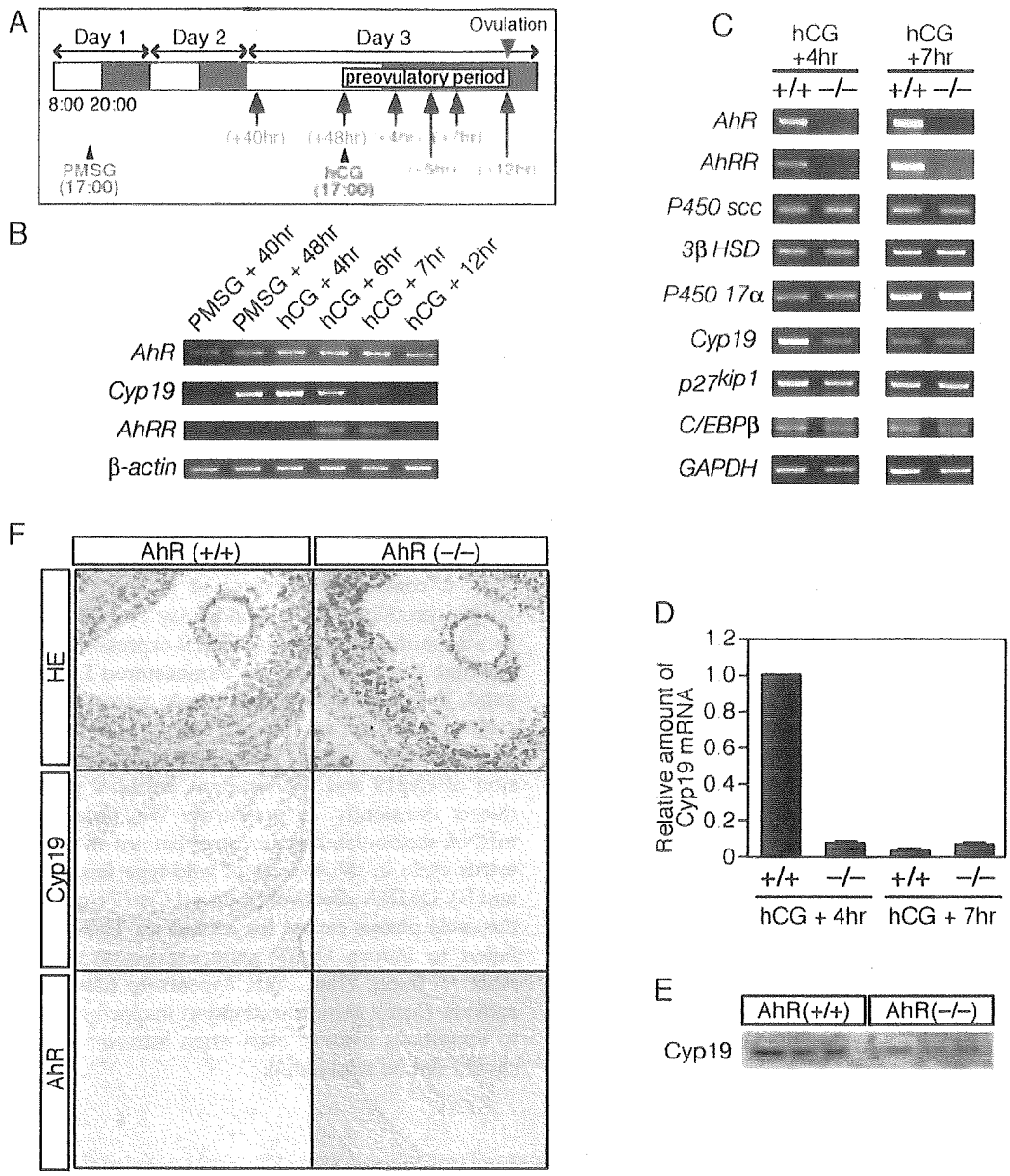

FIG. 4. AhR regulates the expression of ovarian *Cyp19* during the preovulatory period. (A) Schematic representation of the experimental procedure. The estrus cycle was induced artificially by intraperitoneal injection of PMSG at 1700 h on day 1 and of hCG at 1700 h on day 3. Ovaries were collected 40 and 48 h after PMSG injection or 4, 6, 7, and 12 h after hCG injection (indicated by arrows). (B) Profiles of mRNA expression for AhR, AhRR, and Cyp19 during the preovulatory period. Total RNA samples, prepared from ovaries derived from hormone-treated mice at the indicated times (top), were subjected to RT-PCR with primers sets specific for AhR, AhRR, and Cyp19. -Actin mRNA was used as a control. (C) Expression of mRNAs encoding steroidogenic enzymes and proteins involved in ovarian folliculogenesis. Total RNA samples, prepared from the ovaries of hormone-treated AhR / and AhR / mice at the indicated times (top), were used for RT-PCR with the PCR primers. (D) Quantification of Cyp19 mRNA levels. Total RNA samples, prepared from the ovaries isolated 4 and 7 h after hCG injection, were subjected to quantitative RT-PCR analyses. Three animals were used for this experiment. (E) Expression of Cyp19 protein within AhR / and AhR / ovaries during the preovulatory period. Whole-cell extracts (10 g), prepared from the ovaries of hormone-treated (hCG 5 h) mice, were subjected to Western blot analysis with an anti-Cyp19 antibody. Three AhR / and three AhR / animals were used for these experiments. (F) Immunohistochemical staining of Cyp19 and AhR in the granulosa cells of AhR / and AhR / ovaries. Five-micrometer paraffin sections were prepared from the ovaries of hormone-treated (hCG 5 h) mice. Sections were stained with hematoxylin-eosin (HE) or with anti-AhR or anti-Cyp19 antibody.

the Ad4 site of the *Cyp19* promoter and whether the anti-Ad4BP/SF-1 antibody reciprocally precipitates the XRE sequence. Both the XRE- and Ad4-containing sequences of the *Cyp19* promoter were recovered in both anti-Ad4BP/SF-1 and anti-AhR immunoprecipitates (Fig. 6D). As a control, the sequence between bp 2740 and 2441 was not recovered in either the anti-AhR or the anti-Ad4BP/SF-1 immunoprecipitate, excluding the possibility that incomplete fragmentation of

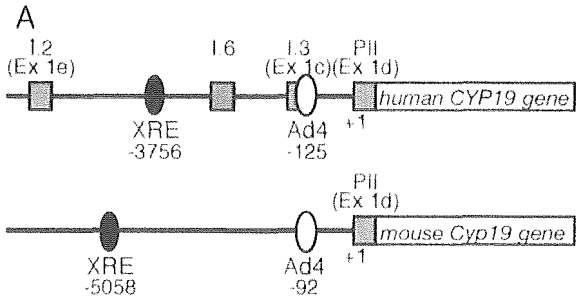

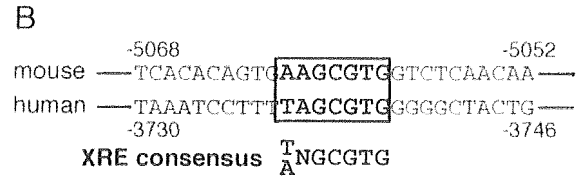

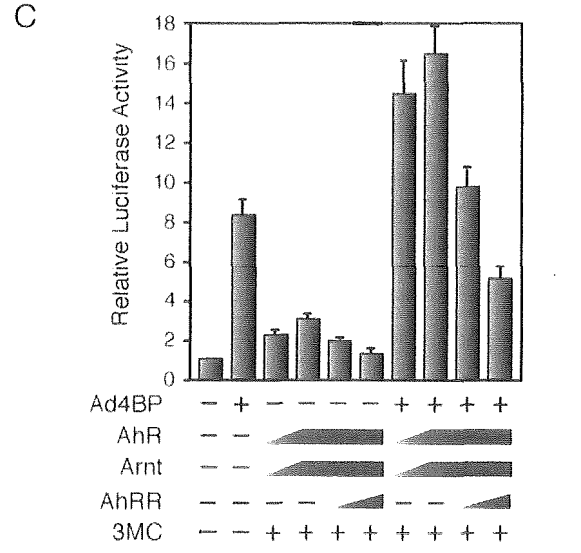

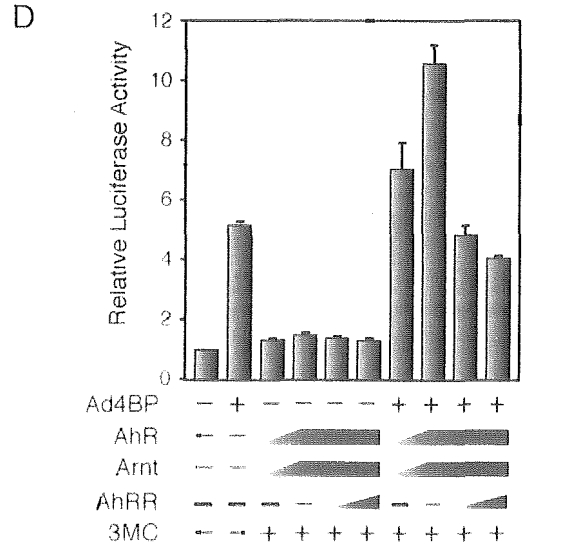

DNA during chromatin preparation resulted in artifactual coimmunoprecipitation of the Ad4- and XRE-containing sequences. To confirm the interaction between AhR and Ad4BP/SF-1 on the *Cyp19* promoter, we investigated whether the XRE is coimmunoprecipitated with Ad4BP/SF-1 in the AhR $^{/}$ chromatin (Fig. 6E). Anti-Ad4BP antibody failed to precipitate the XRE-containing sequence in the absence of AhR, indicating that Ad4BP/SF-1 does not bind directly to the XRE but binds indirectly through interaction with the XRE-bound AhR. In addition, we investigated whether AhR knockout affects Ad4BP/SF-1 binding to the Ad4 site and found that there is no difference in binding of Ad4BP/SF-1 between AhR $^{/}$ and AhR $^{/}$ mice (Fig. 6E). These results clearly demonstrated that both AhR and Ad4BP/SF-1 bind to their cognate binding sites within the *Cyp19* promoter and physically interact, probably leading to cooperative enhancement of *Cyp19* expression.

AhR ligands exerted an estrogenic effect by aberrantly activating *Cyp19* gene expression. While *Cyp19* is expressed transiently at a particular time point in the preovulatory period, AhR is constitutively expressed in granulosa cells. Inadvertently introduced AhR ligands may exert an estrogenic effect by aberrantly upregulating *Cyp19* expression in the ovary. To examine this possibility, we administered DMBA, an AhR ligand, to randomly selected female mice regardless of estrus cycle phase. After a 5-h treatment, we examined the expression of Cyp19 mRNA in the ovary. In a normal estrus cycle, expression of Cyp19 and the resultant estradiol production are induced transiently at proestrus. We observed that Cyp19 mRNA accumulated at proestrus but not at other phases of the estrus cycle in the ovaries of wild-type female mice (Fig. 7A and B). DMBA effectively induced *Cyp19* expression at most of the cycle phases except for metestrus. This reagent, however, failed to induce *Cyp19* gene expression in the ovaries of AhR $^{/}$ mice. Thus, AhR appears to have the potential to activate *Cyp19* gene transcription inappropriately in response to exogenous ligands, even when intrinsic estrogen synthesis should not be stimulated.

FIG. 5. Cooperative activation of AhR and Ad4BP/SF-1 on the *Cyp19*/*CYP19* promoter. (A) Schematic representation of the mouse *Cyp19* and human *CYP19* gene promoter regions. The square boxes indicate the first exons, exons I.2 (Ex 1e), I.6, I.3 (Ex 1c), and PII (Ex 1d), expressed specifically in the placenta, bone, adipose tissue, and ovary, respectively. The filled and open ovals represent the AhR/Arnt-binding (XRE) and Ad4BP/SF-1-binding (Ad4) sequences, respectively. The ovary-specific transcription start site is numbered as 1, and the positions of the XRE and Ad4 sites were numbered as the negative values of their distances from the transcription start site. (B) Nucleotide sequences containing the XRE site from the mouse *Cyp19* and human *CYP19* gene upstream regions. The consensus XRE sequence is indicated in bold letters. (C) Cooperative activation of AhR and Ad4BP/SF-1 on the human *CYP19* gene promoter. Expression plasmids encoding AhR, Arnt, AhRR, and Ad4BP/SF-1 were cotransfected into 293 cells with a reporter plasmid, in which luciferase expression is driven by the *CYP19* promoter (h*CYP19*-3853Luc), in the presence ( ) or absence ( ) of 3MC. After a 48-h incubation, cells were recovered and subjected to luciferase assays. All values are the means SD for three experiments. (D) Cooperative activation of AhR and Ad4BP/SF-1 on the mouse *Cyp19* promoter. m*Cyp19*-5335Luc was used for this assay. All other conditions were as specified for panel C.

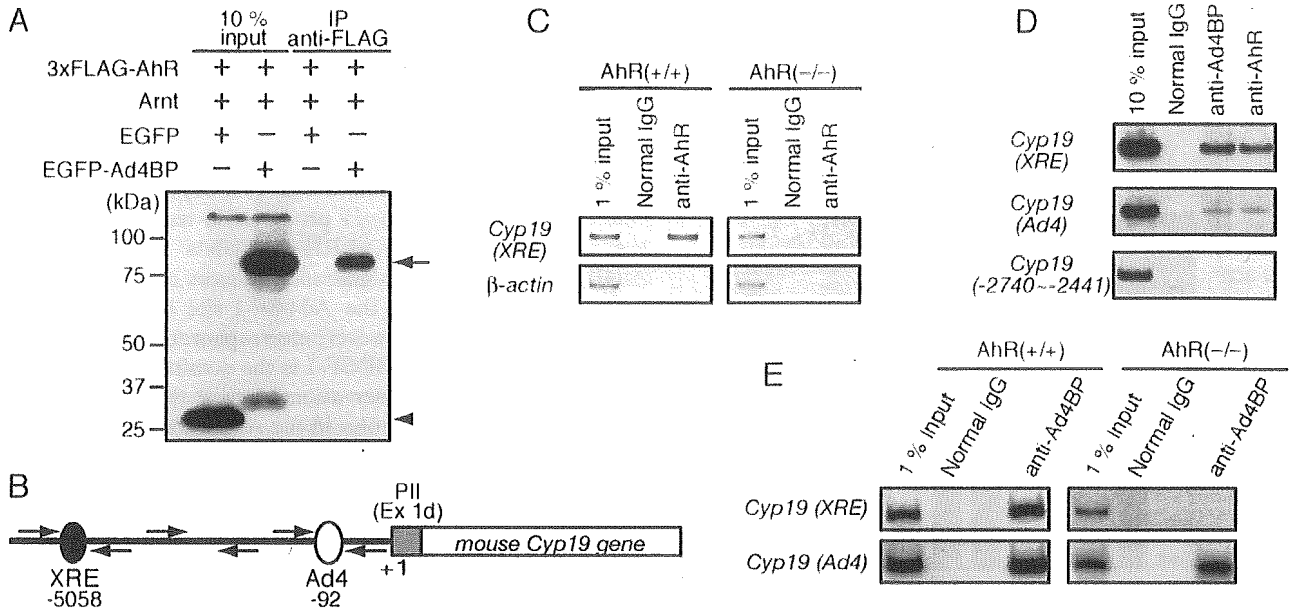

FIG. 6. Interaction of AhR with Ad4BP/SF-1 on the *Cyp19* promoter. (A) Detection of a physical interaction between AhR and Ad4BP/SF-1 by coimmunoprecipitation. FLAG-tagged proteins from whole-cell extracts of 293 cells transfected with 3 FLAG-AhR, Arnt, and EGFP-Ad4BP were immunoprecipitated (IP) with an anti-FLAG antibody. The immunoprecipitates were then subjected to immunoblotting with an anti-GFP antibody. An EGFP expression vector was transfected as a control. An arrow and an arrowhead indicate the EGFP-Ad4BP and EGFP samples, respectively. (B) Schematic representation of the location of primers used in the ChIP assays. Three sets of primers were used to amplify DNA regions containing the XRE site at 5058 and the Ad4/SF-1 sequence at 92 and a third unrelated region (2740 to 2441), containing neither of them, as a control. (C) Binding of AhR to the promoter region of the *Cyp19* gene, revealed by ChIP assays. Soluble chromatin, prepared from preovulatory granulosa cells (hCG 2 h), was subjected to ChIP assay with an anti-AhR antibody. -Actin was used as a negative control. (D) Interaction between AhR and Ad4BP/SF-1 on the *Cyp19* gene promoter. Chromatin isolated from preovulatory granulosa cells was incubated with anti-AhR or anti-Ad4BP/SF-1 antibody and then subjected to PCR with two sets of primers amplifying the XRE and Ad4 sites. A primer pair specific for the sequence from 2740 to about 2441 was used as a control. (E) Binding of Ad4BP/SF-1 to the XRE and Ad4 sites in the presence or absence of AhR, revealed by ChIP assays. Chromatin isolated from preovulatory granulosa cells of the AhR / and AhR / ovaries was incubated with anti-Ad4BP/SF-1 or control antibody and then subjected to PCR to amplify the XRE and Ad4 sites. IgG, immunoglobulin G.

DISCUSSION

In agreement with a previous report (1), AhR / females demonstrated compromised fertility. The number of delivered pups was clearly decreased in comparison to those delivered by wild-type animals. As the phenotype of *AhR* gene disruption suggested a novel physiological function for AhR, in addition to its well-established xenobiotic metabolizing function, we investigated the molecular mechanisms underlying defective fertility in AhR / female mice.

Reproductive defects seen with AhR / female are primarily due to insufficient synthesis of estradiol in the ovary. Abbott et al. described that AhR / females exhibited difficulties in maintaining conceptuses during pregnancy (1), while Benedict et al. reported that AhR deficiency affected follicular maturation and ovulation under normal growth conditions (3, 4). Our studies indicated that follicles present in the ovaries of AhR / mice developed to an antral/preovulatory stage, while the corpus luteum was barely detectable. Upon stimulation of superovulation, the number of ovulated oocytes in AhR / females was significantly lower than those seen with the wild type. In conjunction with the observations of Benedict et al., these results suggested that the reduced fertility of AhR / females was a consequence of ovarian defects during the period of late folliculogenesis to follicular rupture.

Both implantation and follicular maturation are highly dependent on estrogenic action (12). The phenotype of AhR / mice suggested the hypothesis that the observed reproductive failure might be induced by the disruption of genes involved in estrogen production or action. The ovaries of ArKO mice were reported to contain many large follicles filled with granulosa cells, with an absence of a corpus luteum (17). ER KO female mice (14), completely lacking a receptor-mediated response to estrogen, failed to induce preovulatory follicle formation after superovulation treatment. The female reproduction defects of ArKO and ER KO mice resembled those of AhR KO mice, albeit with a more severe phenotype. The similarities between these phenotypes strongly suggested that AhR KO mice have deficits in estrogen production or action. After hypothesizing that estradiol production in the preovulatory period was affected in AhR KO females, we determined that intraovarian estrogen concentrations during the preovulatory stages were decreased in AhR / females. Administration of estradiol increased the number of ovulated oocytes in AhR / females, suggesting that the subfertility of AhR / mice results primarily from reduced levels of ovarian estrogen.

***Cyp19* gene transcription mediated synergistically by AhR and Ad4BP/SF-1.** Ovarian sex steroids, such as estrogen and progesterone, are synthesized from cholesterol through multi-